May 2019

Development of a Resonant High Power Charging Station for Fleet Vehicles

Robabeh Nasiri
University of Wisconsin-Milwaukee

DEVELOPMENT OF A RESONANT HIGH POWER CHARGING STATION FOR FLEET VEHICLES

by

Robabeh Nasiri

A Dissertation Submitted in

Partial Fulfillment of the

Requirements for the Degree of

Master of Science

in Engineering

at

The University of Wisconsin-Milwaukee

May 2019

ABSTRACT

DEVELOPMENT OF A RESONANT HIGH POWER CHARGING STATION FOR FLEET VEHICLES

by

Robabeh Nasiri

The University of Wisconsin-Milwaukee, 2019
Under the Supervision of Professor Robert Cuzner

Conventional vehicles chargers are based on plugging the car battery using wire to the electricity grid through some conversion levels. In general, this system is an interface between the AC grid and the battery which requires DC voltages.

The focus of this research is on wireless power charging technology. The wireless configuration benefits the system by providing electric isolation between transmitter and receiver side, and by making the charging process more convenient for the users.

One major drawback of the wireless charging systems in compare to the conventional system is the lower efficiency of these systems. The resonant high power charging configuration of this study is designed to tackle this problem by enabling soft switching to minimize the switching loss.

In this research a resonant LLC configuration is used for the EV charging application. The configuration and the step by step design of the resonant circuit is illustrated and analyzed. Also, other different topologies of the wireless charging systems have been introduced and compared

with the proposed topology. The converter is modeled and simulated for different modes of operation. The optimal frequency selection which is dictated by the resonant circuit and magnetic design is obtained based on the mathematical model of the circuitry. The simulation results show that the designed converter improves the efficiency significantly using the resonant wireless charging configuration.

Dedicated to my FAMILY for their endless love and support

TABLE OF CONTENTS

LIST OF FIGURES

LIST OF TABLES

ACKNOWLEDGMENTS

I would like to acknowledge my advisor, Professor Rob Cuzner because of his support and guidance.

I also would like to thank Professor Adel Nasiri for his support and encouragement during my education. His guidance and advice have been invaluable throughout all stages of this project and my student life.

I want to thank Professor Saban Ozdemir, Professor Necmi Altin, and Dr. Mehdy Khayamy for helping me with their precious suggestions and comments during this research.

I also wish to thank my committee members, Professor Rob Cuzner, Professor Chiu Law, and Professor Hamid Seifoddini for their time and suggestions.

I would like to thank my mother, brothers and sister whose love and guidance are with me in whatever I pursue in my personal and academic life.

Most importantly, I wish to thank my husband Mohammad who has been my best friend, and great companion in the most positive way during these years.

CHAPTER 1

Introduction

Wireless Power Transfer (WPT) or wireless charging is the technology of transferring power without wires and cables through the magnetic field. In compare to the conventional plug-in power chargers, the WPT technology provides more convenient and safer way for feeding electricity to the electrical devices.

Nowadays, people are using electronic devices in all of the aspects of their lives. The electronic devices are dependent on electricity and they need to be connected directly or indirectly to the electric grid. The conventional electricity grid is designed based on transferring energy using wires and direct plugging of the end user devices to the grid. This method is very efficient and well-known for feeding the electronic devices. However, for some types of applications, it is not very convenient and user friendly. Dealing with the wires and cables in plug-in electronic devices can be hard and time consuming. One of the alternative technologies is the magnetic wireless power transfer which eliminates the need for direct contact of the user with power charging plugs and conductors, and makes the whole charging process safer for the user.

With the increasing interests in the electric vehicles, the electric vehicle charging has become a major area of research in the last decade. The wireless power transfer technology, provide major benefits which with properly to address some of the problems of the EV charging business.

One of the highlighted benefits of the electric cars is the reduction of the greenhouse gases in the atmosphere in comparison with the Internal Combustion Engine (ICE) vehicles. The EVs

benefit the environment by decreasing the air pollution in the areas with large populations. Also, these cars bring some financial benefits, due to the supporting policies by governments. However, the limited range of travel distance and inconvenient charging technologies are the two major issues with the EVs. For example, as shown in table 1, Porsche and Tesla motor's charger that are conventional plug-in chargers, need to be charged for 19 and 50 minutes by efficiency of 93% and 90% respectfully, and there is a limited range of using them before recharging the batteries (the numbers are for the year 2018). There have been some efforts on the other technologies like the wireless charging stations. Qualcomm offers a wireless charger that in this case, the efficiency is lower and charging time of the batteries is more than plug-in chargers [1].

There are many researches going on about wireless charging applications to improve the relatively low efficiency problem of these technology.

Table 1-1. Comparison of existing chargers.

	Tesla	Porsche	Qualcomm
Power	**120kW**	**320kW**	**20kW**
Wireless	**No**	**No**	**Yes**
Charge Time	**50 min**	**19 min**	**300 min**
Efficiency	**90%**	**93%**	**87%**

1.1 Different Type of Cars

1.1.1 Internal Combustion Engine (ICE) Cars

The cars we are using for many years are mainly internal combustion engine vehicles. These cars are fed with fossil fuel and their engines are directly connected to the wheels. Combustion of the liquid inside the cylinder produces a force that will be applied to a piston that results in moving the car. CIE cars have been preferred over steam engine and electric engine cars for years because of their ability and power to work hundreds of miles continuously.

However, the amount of greenhouse gases in the atmosphere produced by the conventional cars is considerable. As the result of that, researchers are investigating the alternative types of cars that are more environment friendly. Hybrid cars that are a mixture of both Electric and ICE cars are a good choice to help decreasing the environmental damage.

1.1.2 Hybrid Cars

Hybrid Vehicles are getting more and more popular these years. These cars are using more than one form of energy and are a combination of an engine that is powered with gasoline (conventional ICE engine), and an electric motor and a battery which allow the gas engine to be smaller and more efficient. They primarily work with gasoline, but the electric engine is also being used. The change of operation between the two source happens based on the multiple conditions. Plug-in Electric Vehicle (PHEV) and full hybrid vehicle are the two types of hybrid cars.

A. HEV (Hybrid Electric Vehicle)

In an HEV you just use the gas engine, but when more power is needed you can move with electric engine. Both the electric motor and gas engine can send the power to wheels at the same

time. The batteries in full hybrid cars are not rechargeable from outside the car and the as motor will move the wheels directly. Using these cars is also more efficient and cost effective because when you stop the car, it shuts the engine off and when you push the brake, it turns on again. This help to save more gas when you are at stop light. The energy from braking charges the battery. [2]

B. PHEV (Plug-in Hybrid Electrical Vehicle)

In the PHEV, the battery of the car is bigger, and you can use the electric engine until it gets discharged completely. International combustion engine can support the engine until the battery gets charged again. PHEVs are rechargeable and can be charged from the grid or gas engine to power the electric motors. PHEVs are cost effective beside being environment friendly. [2]

1.1.3 Full Electric Cars

A Full electric car is completely using electric motor that receives its power from the battery. The battery could be charges from the electrical grid, and also by regenerating the braking energy. Most of these cars can run a range between 80 to up to 250 miles. When the battery is discharged, it takes about 30 minutes (with the fastest charging technology in 2018) and a full day (with the level 1 charging) to get charged again. Using the full electric cars in comparison with the conventional combustion cars can significantly impact the environment and reduce the fuel costs. [2] Figure 1-1 shows a typical diagram of an electric vehicle. The battery is charged from the electric charger and it provides power for the motor, and the wheels.

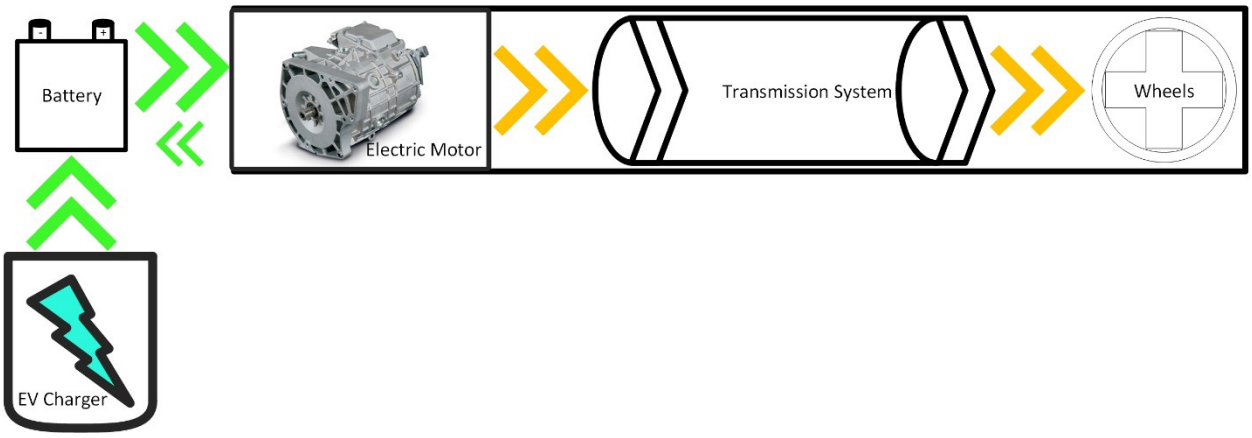

Figure 1-1. Schematic diagram of a typical EV system.

1.2 Different Charging Methods for EVs

1.2.1 Conventional Chargers with Wire

There are several types of chargers for electric vehicles varies. The chargers are classified based on the time of charging and charger's power levels.

Level 1 EV Chargers: This model that is the slowest and cheapest type of the chargers is mostly installed at home or garages. This charger receives AC power, and then converts it to the DC to charge the battery of the car. This type of charger is very convenient to use because users can charge their car by simply plug it into the low voltage household outlet (Figure 1-2). This charger can support 2 to 5 miles per hour of charging and uses 120 V AC (in the U.S.) power outlet with 15 to 20 Amps of current. The maximum power produced by this charger will be 1.9 kW. However, it takes about 7 to 15 hours for the batteries to get fully charged. [3], [4]

Figure 1-2. Standard Household Outlet-Charging

Level 2 EV Chargers: Figure 1-3 is a picture of charger level 2. The level 2 chargers could be used for charging stations at home or public places. This charger needs a 208/240 V AC for supporting 10 to 20 miles per hour of charging with the power rating of 19.2kW while the single phase or three phase AC mains will not exceed 80 Amps. This type of charger needs 3 to 5 hours for full charging. Level 2 in comparison with the Level 1 needs more safety consideration for connecting to the grid and ar. Figure 1-4 shows a schematic of the level 2 chargers with the connector and control devices connected to the grid. it is very similar to the level 1 chargers [3], [4].

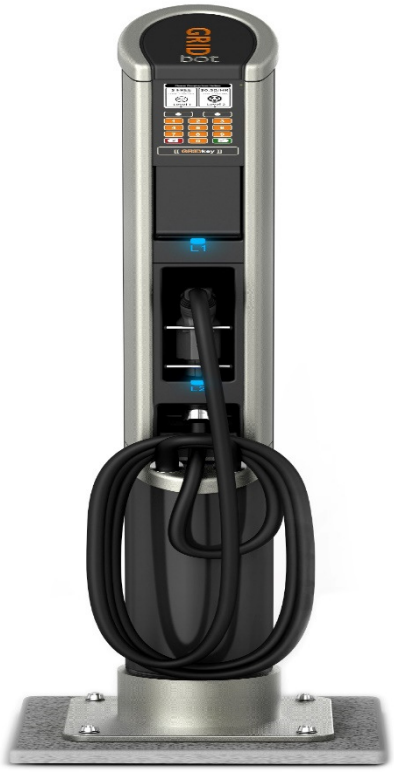

Figure 1-3. A picture of Level 2 charging station

***Level 3 EV Chargers*:** This type of chargers that is also known as DC Fast Charger requires 480 V AC for supporting up to 50 kW in less than one hour for 60 to 80 miles. It is currently the fastest way of charging. DC fast chargers which are mostly used in public stations work with an off-board charger that will convert the AC voltage to DC using a rectifier. The battery in the car gets the DC power directly from the station. Tesla has its own DC fast charger that is called supercharger. Figure 1-5 is a picture of the DC fast charger [3].

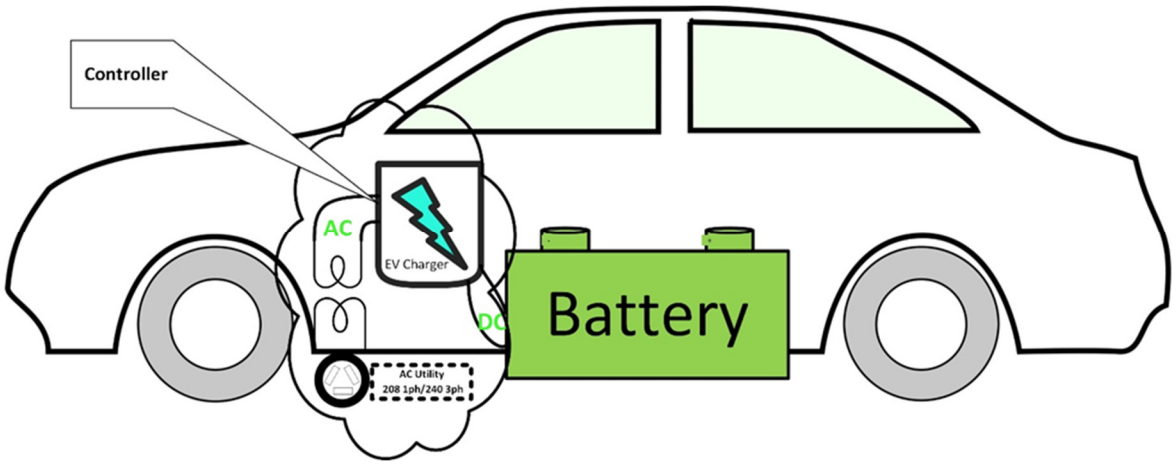

Figure 1-4. Schematic of an electric vehicle charging system.

Figure 1-5. A picture of a DC fast charger.

1.2.2 **Wireless Chargers:**

In this type of chargers, there is no need for connector and cord between the charging station and vehicle while the power is being transferred. The charging happens through an electro-magnetic field. The charging system as t is shown in figure 1-6 includes two pads, transmitter that is a part of the charging station and receiver that is installed in the EV. The transmitter and receiver coils are inside these two pads. Although wireless chargers are safer and more convenient in

compare to the wired chargers, low efficiency and long charging time of these chargers, make the users uninterested. However, with increasing researches on improvement of this type of power transfer, wireless chargers are improving to become a better choice in the future. Many companies such as Qualcomm, Toyota, and GM have been working on the wireless charging technology for EVs and many researchers are pursuing this topic to address the drawbacks of the Wireless Power Transfer (WPT) applications.

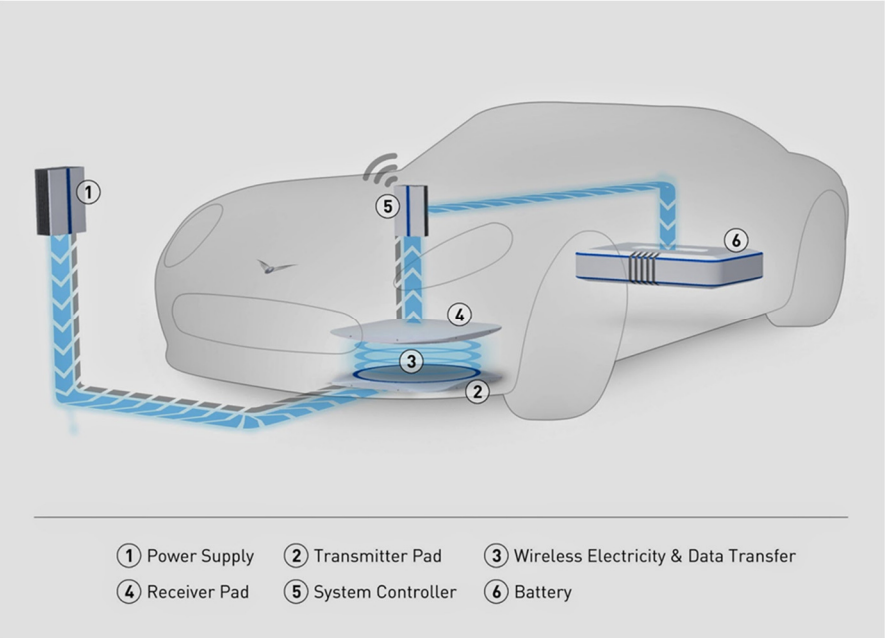

Figure 1-6. A picture of wireless charging system

1.3 Plug-in Charger VS. Wireless Charger

Currently, the most common and practical way of charging are plug-in chargers. The electric power transfers through the wires between the plug and battery of the car after some conversion levels. However, there are some disadvantages with the wired chargers. For instance, there is a chance of electrocution with the plugs especially in the wet environment, and the long wire may cause safety issue. In addition, during the bad weather condition with snow and ice, the plug and

cables may get frozen. However, wireless power charging can be a solution for these problems that wired chargers may encounter. Wireless charging that allows the batteries to get charge through the magnetic field are safer because of the galvanic isolation between the battery in the car and the charger. Wireless chargers are also more practical in bad weather condition.

Wireless charging can be built in large the scales for public transportation like public buses. Buses can get charged while parked in the parking area and this availability of excessive charging places during the working hours can practically reduce the battery packs. Vehicles can get charged whenever they are stopped which could result in reducing the car's weight and volume [5].

1.4 Thesis Outlines

The researches in the area of wireless EV chargers are focused on improve the efficiency of the system which is a significant problem in the wireless charging [6-8]. In general the tong charging time of the batteries that is an important case in EV chargers (wired and wireless) can be solved by lowering the loss of the whole charging system and increasing the efficiency. The efficiency is a more significant challenge for the wireless technology do to the loss of power in the power transfer between transmitter and receiver.

The goal of this research is to design and simulate an efficient topology for the wireless high-power EV charging station that is capable of generating 330kW power to the output in a reasonable amount of time. Table. 1-2 shows the parameter specification of this system. In order to get a better efficiency and reduce the size of the system, a 330-kW resonant LLC converter is proposed. This soft switching can decrease the switching loss and improve efficiency significantly. In addition, high frequency design of the magnetic part that is a part of the LLC resonant converter

is smaller than the regular low frequency designs which reduces the overall size of the charging system.

Table 1-2. System parameters specification

Item	Rating	Unit
Input Voltage	600-800	V
Output Voltage	350	V
Output Power	330	kW
Resonant Frequency	30	kHz

Combining the grid connected system with energy storage, the systems can feed the output during heavy loads and when the system load is lighter, the energy storage can get charged during the light or no load conditions. This thesis will discuss most of the significant points that are necessary to model and design an LLC resonant converter.

Chapter 1 includes the literature review and an introduction of the different existing charger's levels. A comparison of wireless power charger and plug-in charger is also included in this chapter.

Chapter 2 is providing an overview of the different wireless power transfer technologies and their power level. At the end of the chapter, the existing wireless chargers and researches are reviewed.

Chapter 3 is an introduction of the conventional resonant converters and their advantages and disadvantages. The component selection of the LLC resonant converter is also illustrated in

this part. In addition, the mathematical model and different modes of operation of the selected converter is discussed in this chapter.

In chapter 4, the discussion is on the control of the different parts of the circuit. A

Chapter 5 includes the simulation results and their analysis. The voltage and current waveforms of the LLC resonant converter and their behavior in different modes of operation have been discussed.

Finally, chapter 6 is a summary of the thesis and the work performed on the different parts of the project.

CHAPTER 2

Wireless Charging System Topologies

The battery charger is an essential component of an electric vehicles. The AC power from the grid is converted to DC, and then gets adjusted to the proper voltage of the car battery. Normal plug-in chargers are using a cord to get connected to the car. Generally, transferring power with the cables in short distance is very efficient. On the other hand the wireless power transfer system has more conversion levels including electromagnetic conversion which reduces the efficiency. This efficiency in the new developed wireless technologies for the short distance is still in an acceptable range.

Charging time and effect on the battery life time are two of the most important factors in the popularity of EV chargers. High efficiency, high power, low volume, low weight and being safe for the user are the other important requirements. In this section, different type of wireless power transfer, their characteristics, and their suitability for EV chargers is discussed.

2.1 Wireless Power Transfer

Wireless power transfer is defined as transferring power between transmitting coil to the receiving coil through the magnetic field without any cables or wires involved. Wireless power transfer is used in some applications like portable devices, some medical devices. The focus of this research is on studying the WPT for the EV chargers. Figure 2-1 shows the general structure of

the wireless power transfer systems. The receiver is placed in the secondary side and is connected to the load. The transmitter is in the primary side of the system. The transmitter is fed by the main component of the system that are connected to the grid or power sources. The transmitter and receiver are electrically isolated. Each of the transmitter and receiver sides have an AC/DC power converter [1].

There are several configurations of WPT technology. Different types of WPT, their advantages and disadvantages, and most importantly their suitability for wireless battery charger for electric vehicles is discussed in the following section.

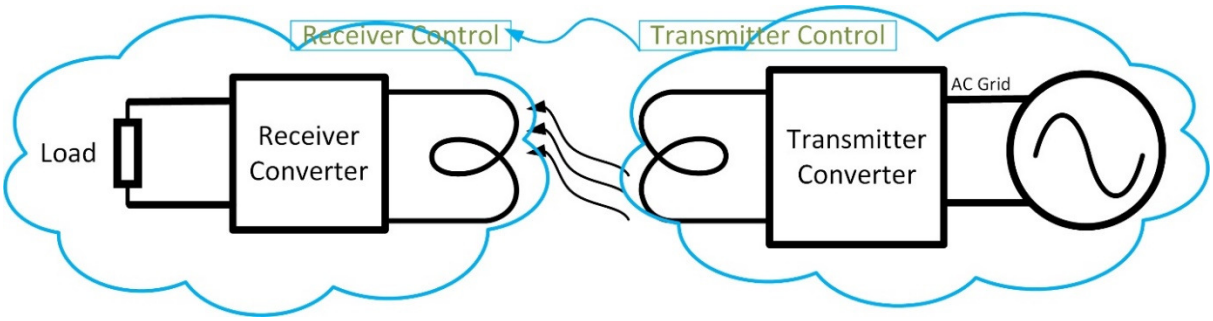

Figure 2-1. Wireless power transfer structure.

2.2 Classification of Wireless Power Transfer

Figure 2-2 categorizes the various types of WPT and their applications. This technology can be divided into three big categories; electromagnetic field, magnetic gear, and capacitive power transfer.

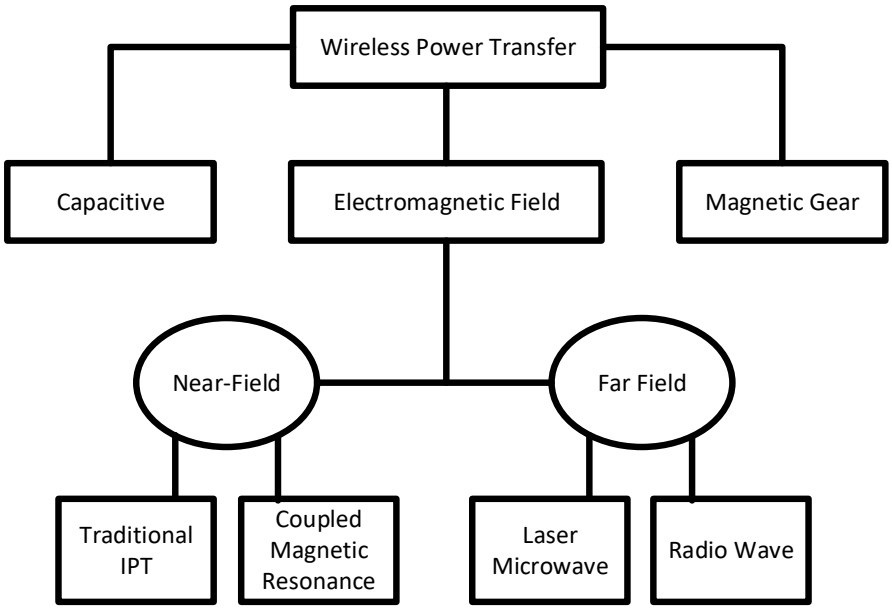

Figure 2-2. Classification of wireless power charging technologies [9].

2.3 Comparison of Different Types of Wireless Power Transfer

Table 2-1 shows the comparison between different types of wireless power transfer technologies. Capacitive wireless Power transfer(CWPT), Magnetic gear wireless power transfer(MGWPT), Inductive power transfer (IPT), and Resonant inductive power transfer(RIPT). The last two categories are two different types of electromagnetic fields WPT. The last row of the table discusses the suitability of each group for the wireless electrical vehicle's charger application.

Table 2-1. Comparison between different types of wireless power transfer technologies [10].

WPT methods	Inductive	Capacitive	Resonant inductive	Permanent Magnet
Efficiency	**Medium/High**	**Low/Medium**	**Medium/High**	**Low/Medium**
EMI	**Medium**	**Medium**	**Low**	**High**
Frequency range(kHz)	**10-50**	**100-600**	**10-150**	**0.05-0.500**
Price	**Medium/High**	**Low**	**Medium/High**	**High**
Size/Volume	**Medium**	**Low**	**Medium**	**High**
Complexity of design	**Medium**	**Medium**	**Medium**	**High**
Power level	**Medium/High**	**Low**	**Medium/Low**	**Medium/Low**
Suitability for WEVCS	**High**	**Low/Medium**	**High**	**Low/Medium**

2.4 Capacitive Wireless Power Transfer (CWPT)

Capacitive wireless power transfer is suitable for the low power applications such as portable devices and cellular phone chargers because of its low cost and simplicity. This technology can transfer power through the AC electric field. Figure 2-3 shows the schematic of CWPT. In the CWPT, instead of using magnet or coil, coupling capacitors are transferring the power from the transmitter to the receiver. The high frequency AC power that is produced by the H-bridge will go through the coupling capacitors, and then to the receiver side. The inductor in

series with the coupling capacitor between the transmitter and receiver will lower the impedance and enable soft switching. The battery pack at the end receives the DC power converted by the rectifier as it is shown in the figure.

The power transfer rating of the converter depends on the air gap between two plates and the size of coupling capacitance. Because of the small size of coupling capacitance, CWPT technology might face practical problem in real application. CWPT works better when the distance between the plates is small. Any air gap between two plates and any displacement of coupling plates will decrease the capacitance. As a result, CWPT is impractical for Wireless EV charging with 150-200 mm air gap or higher, or for the situation with potential large displacement, and for the high power level WPT systems [10], [11].

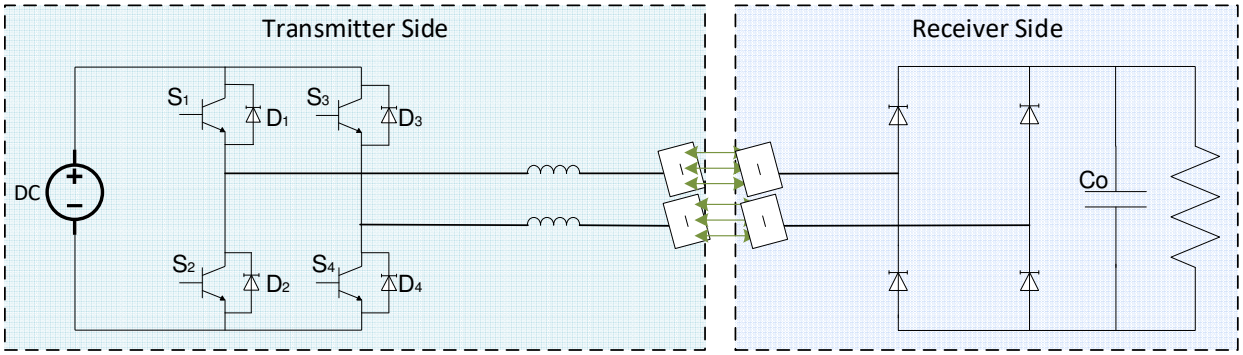

Figure 2-3. Schematic of capacitive wireless power transfer [10]

2.5 Magnetic Gear Wireless Power Transfer (MGWPT)

Magnetic gear wireless power transfer uses mechanical forces to transfer power through the system. Magnetic gear, is used in some applications such as EV motors and wind power generators instead of conventional contacted gear. It has also been used in low power medical implants such as cardiac pacemaker, and high power application of vehicles and electronics. Figure 2-4 shows the general schematic of the MGWPT.

In this technology, two synchronized permanent magnets are used as the main coupling mechanism that is positioned side by side rather than coaxial in contrast to the other common applications in EV and wind generators. The input of the transmitter winding is a current source which produces an electro- mechanical torque on the primary side. The PM in the primary side rotates, and causes the rotation in the secondary side with the same speed as the transmitter PM. In this process, the battery gets charged by a rectifier which is shown in the figure. Primary side PM works at the generating mode and sends power to the secondary PM and then to the car battery [10].

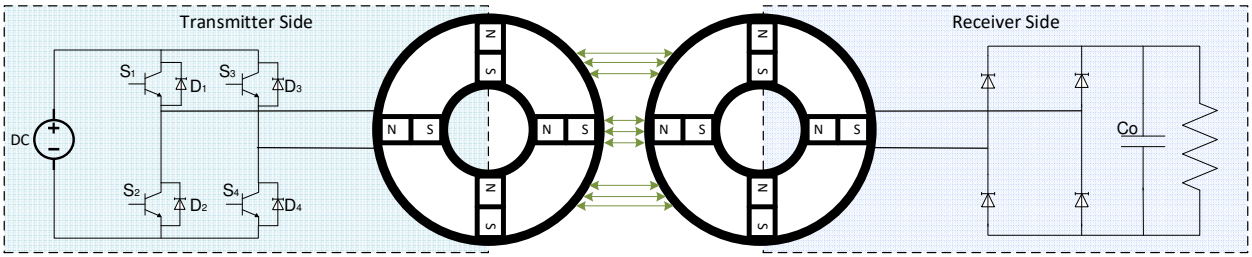

Figure 2-4. Schematic of magnetic gear wireless power transfer [10].

2.6 Electromagnetic Field WPT

Wireless power transfer is classified into two types of near field and far field based on the air gap between transformer and receiver.

2.6.1 Near-Field and Far-Field

In the near field that is also called non-radiative power transfer, the distance should be less than one wavelength. One important example of the near field is inductive power transfer that is used in the induction motors. Charging technology of electronic devices such as toothbrush and cell phones are other examples of the near field power technology. Efficiency and power transfer

in the near field are highly affected by the air gap, and as the distance increases the power transfer decreases ($1/r^3$). As the result in this method keeping the operating range below several centimeters is crucial. This operating range and the efficiency of the system can be extended in the coupled magnetic resonance technology because of the resonance circuit [12].

In contrast, in the radiative or far field power transfer, the power can be transferred from the length as big as the wavelength to infinity. Laser, microwave, RF, and photoelectric are examples of the far field technology. The operating range of far field is more than several kilometers with the very high frequency range (kHz-MHz). Far field charging is not applicable for the EV charging [12].

2.7 Inductive Power Transfer (IPT)

Figure 2-5 shows the block diagram of the induction power transfer. IPT was first improved by Nikola Tesla in 1914 [12]. In this technology the power is transferred between the transmitter and receiver that are two coils coupled in a magnetic field. The first coil gets excited with the AC voltage and makes the second coil excited by generating magnetic field. Then, the power is sent to the battery by the receiver after rectification [3]. This technology offers a convenient, and low cost solution with an adjustable range of power transfer with the flexible inductive coupling design. Even though the inductive wireless power transfer is an efficient power transfer technology in small distances, the losses over the coil resistance are considerable.

Some challenges are important to be considered in this technology that has a wide range of power transfer from mWatt to kiloWatt. Charging control strategy, coil design, magnetic structure and alignment of the windings are the parts that should be considered and controlled in order to meet an efficient and safe power transfer [13], [14].

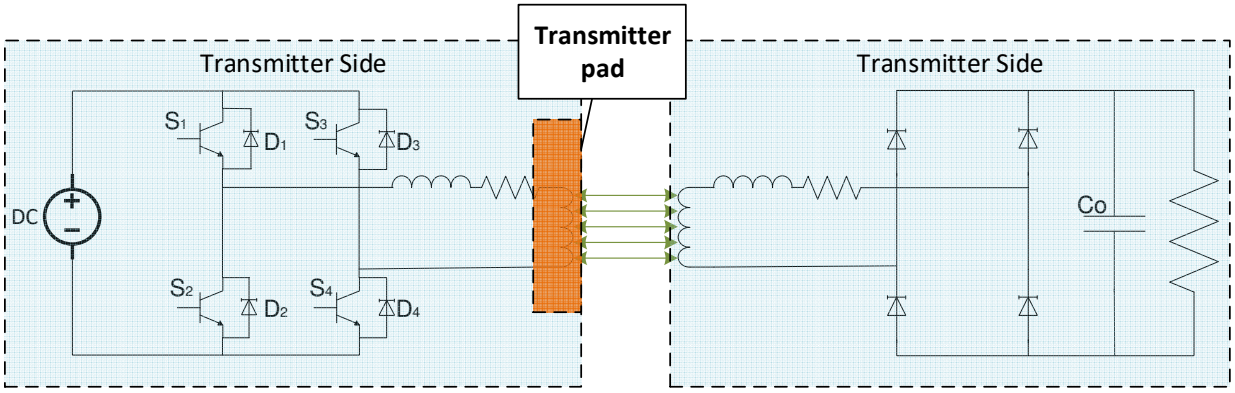

Figure 2-5. Traditional inductive wire power transfer [10].

2.8 Resonant Inductive Wireless Power Transfer (RIWPT)

Resonant inductive power transfer is the improved version of the inductive wireless power transfer and a kind of Near-field WPT technology. In this technology, one capacitor is added to the primary and secondary side of the coupling coil in traditional IPT in order to increase the efficiency of the system and increasing the power transfer distance (Figure 2-7). Also, high frequency AC voltage in the first part goes to the winding, and then to the secondary winding through the magnetic field. The battery bank of the EV at the end receives the DC power converted by the rectifier and filter circuitry.

The capacitor is charged by the current produced in the magnetic field over the inductor winding. Then the capacitor discharges and generates current to produce magnetic field over the inductor again. This causes power transfer between the capacitor and inductor. [10]

The capacitors also can affect the transmitter side by decreasing the reactive power and increasing power transfer to the load in the receiving side of the system. Equation (2-1) shows how the resonant case is created in this topology. Fr is the resonant frequency on the primary and the secondary side. The self-inductance L and resonant capacitor C in the primary and secondary side

resonate and when the resonant frequency in the two sides are matched the efficient power transfer happens. The frequency range in this model is between tens of kilohertz to several hundreds of kilohertz.

Coupling coefficient in the EV system is a small value like 0.2 or 0.3 duo to the height limitation of the transformer parameters. Coupling coefficient can be calculated using the equation (2-2) [10].

$$f_{r(P,S)} = \frac{1}{2\pi\sqrt{L_{p,s}C_{p,s}}} \quad (2\text{-}1)$$

$$k = \frac{L_m}{\sqrt{L_p L_s}} \quad (2\text{-}2)$$

L_m is the magnetizing inductance of the two coils. Larger values of L_m are the results of the coupling coils that are strongly coupled together. L_p and L_s are the self-inductance of the primary and secondary coils. [4]

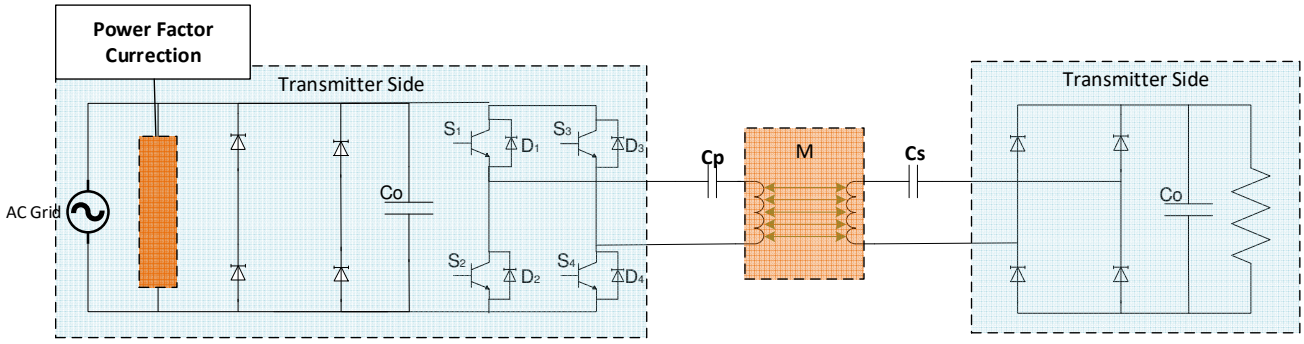

Figure 2-7 Resonant inductive wire power transfer [10].

2.9 Compensation Network

Large leakage inductance and small mutual inductances on the transformer's coils will reduce the power transfer capacity of the inductive wireless power transfer technology. In order to compensate the coil's leakage inductances to create bigger mutual inductance, compensation

capacitors are needed. Compensation capacitors can be added to the primary and secondary part of the coupling coils in series and parallel combinations to get a higher power transfer and lower loss. Four different topologies can be derived from these combinations as it is shown in the figure 2-6 that are series-series (SS), series-parallel(SP), parallel-series(PS) and parallel-parallel(PP) [15], [16].

When the primary side is in series, it can help reducing the power source voltage while the parallel-compensated primary can support more supply current. The series–compensated secondary is better for constant voltage applications and parallel-compensated topology is suitable for the constant current circuits. As a result, the secondary side compensation is required to maximize the load power transfer and efficiency while the transmitter side compensation network is required to minimize the reactive power in the source. Different compensation topologies have their advantages and disadvantages and choosing the good topology is depending on the application that has been discussed in the table (2-2).

The SS topology in figure 2-6 that is similar to the circuit of the resonant inductive wireless power transfer, has been discussed in the previous section. This topology has been considered in researches as the best topology for the EVs application because of the independency of the capacitors in the first and second side of the transformer to the load condition and mutual inductance. In addition, these topologies can keep the unity power factor by drawing active power at the resonant frequency [10], [15], [16].

Misalignment between coils can interrupt the power transfer to the output. While the PS and PP topologies provide a safe environment during the power transfer. Since the primary coil

does not operate in the absence of the secondary coil, higher power level might not be achievable at the output when the misalignment happens between two coils. [3].

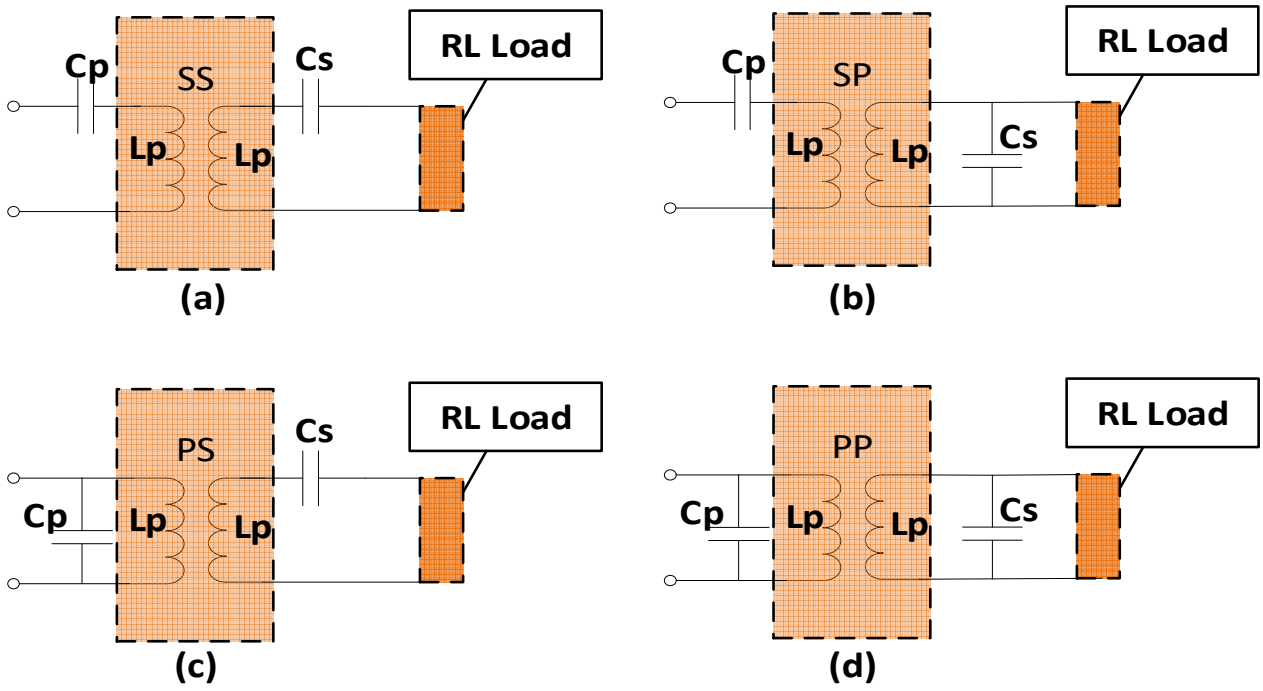

Figure 2-6. Different topology of compensation network [10], [15].

Table 2-2. Comparison of different compensation network [10]

Features	Series-Series(SS)	Series-Parallel(SP)	Parallel-Series(PS)	Parallel-Parallel(PP)
Power Transfer Capability	High	High	Low	Low
Sensitive of Power Factor Over Distance	Less	Less	Moderate	Moderate
Alignment Tolerance	High	High	Moderate	Low
Impedance at Resonant State	Low	Low	High	High
Frequency Tolerance on Efficiency	Low High	High	Low	High
Suitable for EV application		High	Moderate	Moderate
Primary Capacitor	$\frac{1}{\omega^2 L_p}$	$\frac{1}{\omega^2(L_p - \frac{M^2}{L_s})}$	$\frac{1}{\omega^2(L_p + \frac{\omega^2 M^4}{L_p R_{Load}})}$	$\frac{1}{\omega^2(L_p - \frac{M^2}{L_s} + \frac{\frac{M^2}{L_s^4}R_{Load}^2}{\omega^2(L_p - \frac{M}{L_s}}$
Secondary Capacitor	$\frac{1}{\omega^2 L_s}$	$\frac{1}{\omega^2 L_s}$	$\frac{1}{\omega^2 L_s}$	$\frac{1}{\omega^2 L_s}$
Load	$\frac{\omega L_s}{Q_s}$	$\omega L_s Q_s$	$\frac{\omega L_s}{Q_s}$	$\omega L_s Q_s$

2.10 Wireless Battery Chargers

The basic structure of a magnetic wireless battery charger is an AC/DC converter which is directly connected to the grid. The first section of the converter converts AC to DC. Then using a DC/AC converter to feed the transmitter. The compensation network in the two sides of the system are helping to achieve a better efficiency from the system. The magnetic flux will go through the coils from transmitter to receiver that is placed in the electrical car and is a part of the whole battery chagrin system. The battery receives the DC power and is charged from an AC/DC converter that is connected to the receiver at the end of the line [16].

The power control, communications, and battery management system (BMS) are also necessary, to avoid any health and safety issues and to ensure the stable operation [15].

2.11 Applications of Wireless Battery Charger

Figure 2-7 shows a general stationary wireless EV Charging System. The vehicle gets charged through the primary and secondary pads while it is parked in a parking. The first pad that is installed underground which includes the transmitter and power converters. However, the receiver is a part of the vehicle that will be installed in the front, center or back of the car. The system includes a power control logic to avoid any problem.

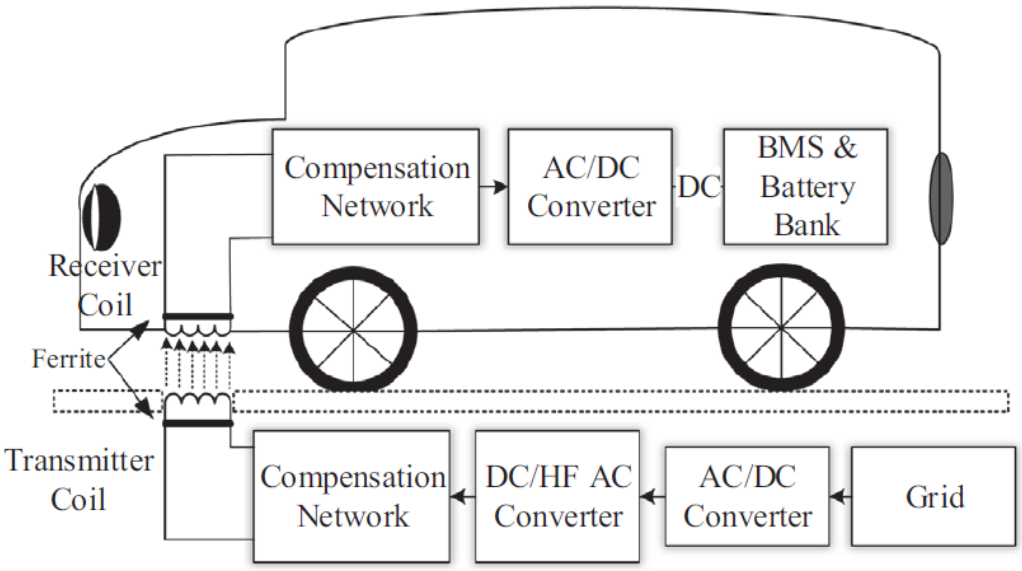

Figure 2-7.General diagram of the static wireless power charging of EVs [10].

Efficiency, maximum charging distance, vehicle's weight and charger's power level are the main characteristics that are considered in the design of EV chargers.

There are several researches on optimizing the design and developing an efficient inductive wireless power transfer topology. These efforts help the designer to achieve lower loss and lower charging time.

One of the most famous existing wireless chargers belongs to QUALCOMM. "Qualcomm Halo WEVC" technology uses resonant magnetic induction to transfer energy between a ground-based pad and a charging pad on the electric vehicle. The Base pad and the vehicle pad are magnetically coupled and tuned, and energy is transferred efficiently between the pads. Power is converted to DC using an on-board converter to charge the vehicle's batteries. The charging power level are 3.3kW, 6.6kW and 20 kW with the efficiency of 87% [18].

There is also a famous product which is introduced by WiTricy Corporation. This family of wireless charger systems offer the power rating of 3.6-11 kW with the interesting efficiency of greater than 90 %.

There is also a developed product from Siemens and BMW jointly which claims the efficiency of more than %90 for transferring 3.6 kW of power.

These products are developed mainly for the application of charging small passenger cars. The physical distance between the transmitter and receiver of these introduced examples are between 80 to 250 mm. Several other efforts by industries are almost in the same range of efficiency and power ratings [13].

Some companies like conductive dynamic are working on the WPT for E-Bus for transferring around 30 kW of power, and higher coil's distance of around 300 mm.

In the scale of university and research centers, the developed prototype by KAIST university and university of Michigan Dearborn have reached the claimed efficiency of almost 95-96 present [17].

2.12 The Illustrated Topology of This Project

The studied topology of this research is a part of a grid connected charging station for EVs. As it is shown in figure 2-8 the system is rated for 330 kWh power rating. The first DC bus after the grid connected inverter is considered as the bus for connecting a battery system with 110 kWh capacity to support the grid for supporting the system in the peak time.

The input rectifier is designed as a bi-directional active converter that can support the grid by providing the active and reactive power from the DC busbar at the grid side. However, the HF

resonant converter of the core of this system is a one directional converter with a diode rectifier stage. The design, modeling and control of the converters of this system and the resonant tank will be illustrated in detail in this thesis.

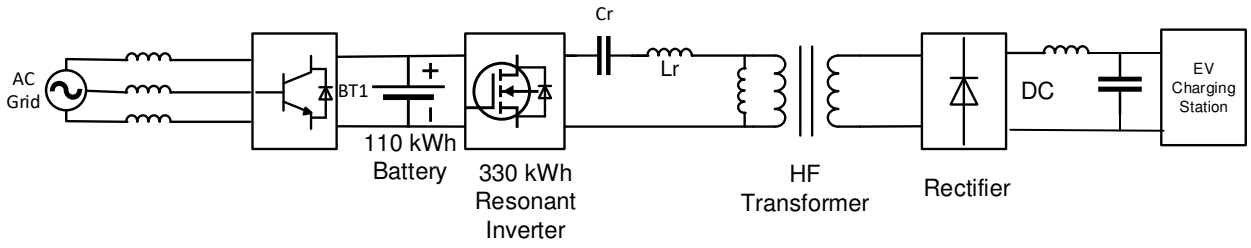

Figure 2-8. 330kW Wireless EV Charger (WEVC) Topology

.

CHAPTER 3

Resonant High Power Wireless Charging Concept

Due to the economic and environmental considerations, using electric vehicles is becoming more and more interesting for the costumers around the world. Using the electric vehicles for transportation in the cities, the fossil fuel burning for energy generation could be moved out of the cities and the places with human population. In general, the large scale fuel based power plants are more efficient and cost effective. Also, the air pollution which is caused by burning the fuels could be dealt with in a much effective way in the power plants in compare to the multiple vehicles which are distributed everywhere. Besides, the latest technology advancements in making the energy storage systems and renewable energy-based electricity more efficient and cost effective [19], which could ultimately be used to generate and store energy for the EVs with huge relative cost reduction.

The electrical vehicle concept and technical studies are focused on three major areas; electrical engine and converters inside the car, energy storage systems (batteries) and the charging systems. The focus of this study is on the EV charging system and studying an innovative charging configuration for convenient, efficient and faster charging of the batteries.

The topology of this research is a resonant high power wireless charger which eliminates any need for physical contact between the EV and charging station. It enables more convenient and safer charging; besides, using resonant power electronic conversion in this topology, soft

switching in the PE converters is enabled which improves the system efficiency and reduces the generated heat in the whole process.

3.1 Resonant Converters

Switch mode converters have the problem of high switching power loss and high switching stress, since they are required to turn on and turn off at full power during each switching cycle. This problem will be more highlighted by increasing the power and switching frequency of the switches. Therefore, for enabling the application of the high frequency that leads to the reduction of the converter's size and weight, some techniques like application of resonance converters is necessary to help to keeping the efficiency and power rating high. In the resonance topology a form of LC resonance will be added to the converter in order to shape the waveforms of voltage and/or current during the switching transition when the voltage across it or the current through it is zero. A Zero Current Switching (ZCS) circuit shapes the current waveform, while a Zero Voltage Switching (ZVS) circuit shapes the voltage waveform that are the results of combination of switching strategies and converter topologies.

Series- Loaded Resonant converter (SLR) and Parallel- Loaded Resonant converter (PLR) are two types of resonant converters that are classified based on their circuitry. In the SLR configuration the resonant tank capacitor is placed in series to the load while in PLR, the capacitor is in parallel to the load [8]. The SLR and PLR topologies are benefiting from a LC resonant tank to create conditions for lossless turn-on or turn-off of the switches and providing zero-voltage and zero-current switching.

3.2 Series-loaded Resonant DC-DC Converters

Figure 3-1 shows the configuration of Series-loaded resonant converter. The name of this converter comes from the arrangement of the capacitor and inductor (Resonant Tank) that are in series with the output load. The isolation transformer in this configuration also helps with the regulating of the output voltage. The output voltage can be affected by the filter capacitor C. Therefore, choosing a big capacitor can help in reducing the ripple of the voltage across it. The voltage at the secondary side of the transformer is fed to the rectifier. This magnitude of this voltage is V when the inductor current is positive and –V when the inductor current is negative.

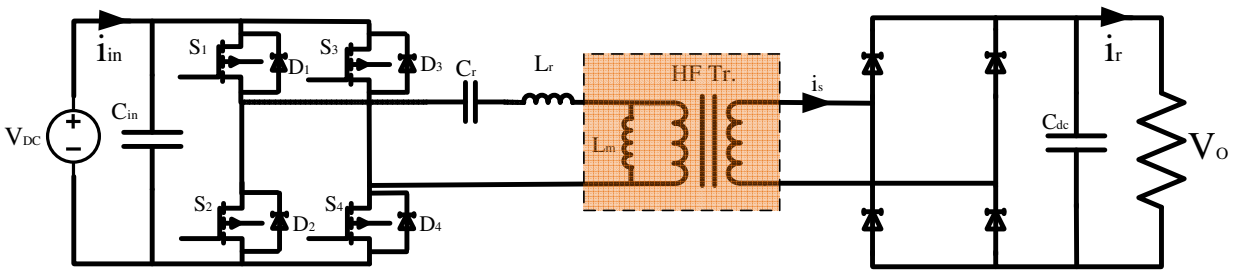

Figure 3-1. Series Loaded Resonant converter [24].

The voltage across the LC tank is dependent on the inductor current condition and the switches. When i_L is positive and the switches Q_1 and Q_4 are on, the inductor current flow through the Q_1 and Q_2. However, when the switches are off, the current conducts through the diodes D_2 and D_3. On the other hand, when i_L is negative, it flows into the switches Q_2 and Q_3 if they are conducting, otherwise it goes through the diodes D_1 and D_4. Figure 3-2 is the equivalent circuit of the Series-Loaded Resonant Converter.

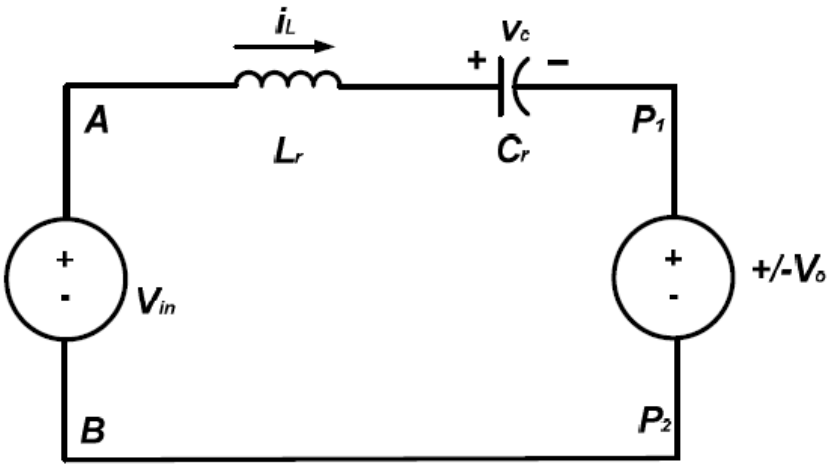

Figure 3-2. Equivalent circuit of series-loaded resonant converter

This topology has three modes of operation that are determined by the ratio of the switching frequency $f_s = \omega_s/2\pi$ to the resonant tank frequency $f_0 = \omega_0/2\pi$. The three modes of operation have their advantages. When the $\omega_s < 1/2\omega$ we can have the natural zero current switching. In mode 2, when $1/2\omega_0 < \omega_s < \omega_0$, we can achieve both ZVS and ZCS switching. The third mode $\omega_s > \omega_0$, gives us the chance of having natural zero voltage switching. This can help the converter to reduce turn on loss and turn off loss during the switching transitions [24].

3.3 Parallel Loaded Resonant Converter

The main difference in the configuration of the Parallel-Loaded Resonant Converter (PLR) with the SLR is that in the PLR, the resonant tank consists of a capacitor and inductor while the capacitor is in parallel with the output load. This topology that is working as a voltage source can step up or step down the voltage and it is a proper configuration for the converters with variable output voltages.

The configurations below show the Parallel-Load Resonant converter and its equivalent circuit. PLR has an inductor before the output capacitor. The voltage across the load is filtered by

the capacitor and the current through the filter inductor can be assumed as a ripple free current because of the high switching frequency and the large inductor filter.

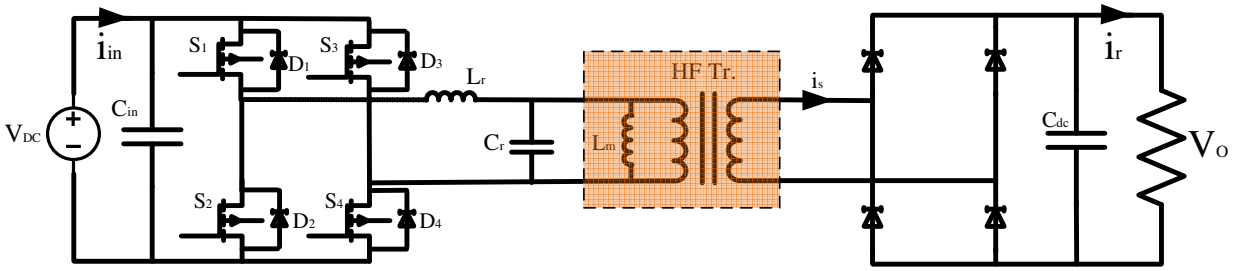

Figure 3-3. Parallel-Loaded resonant DC-DC converter [24].

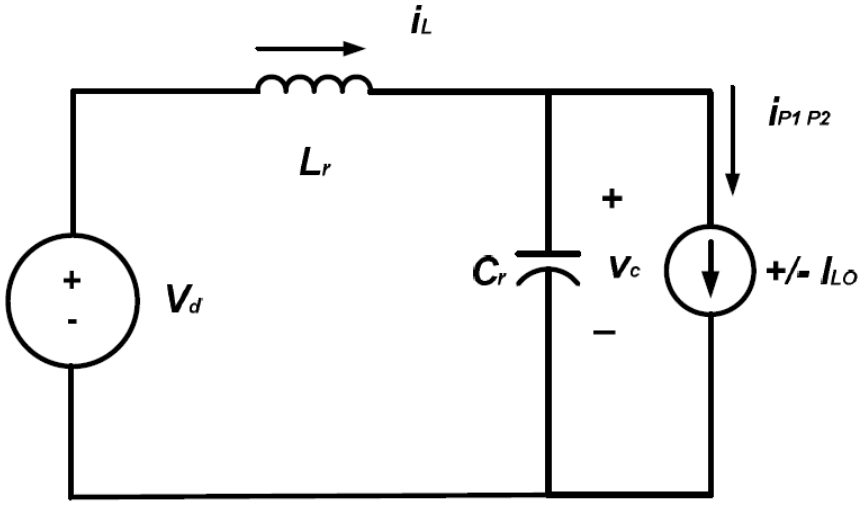

Figure 3-4. Series resonant converter with Parallel-Load equivalent circuit

3.4 LLC Resonant Converter

LLC converter is a part of the resonant converter family that consists of a series capacitor (C_r), a series inductor (L_r) and a parallel Magnetizing inductor (L_m) in the resonant tank part. The configuration below shows a full bridge LLC converter with a full bridge rectifier. The resonant tank gets receives a square waveform generated by switching bridge. The current in resonant tank is sinusoidal. The voltage is finally rectified in the rectifier and builds the output DC voltage [26].

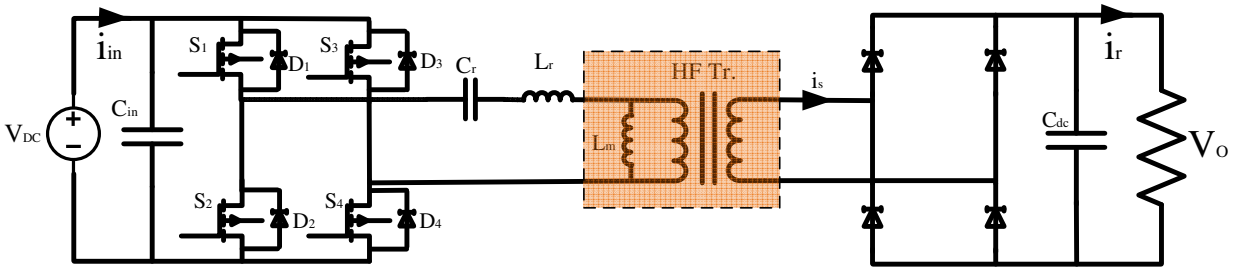

Figure 3-5. LLC resonant converter [24].

There are two resonant frequencies for the whole operation that are important to notice. One frequency that is the result of the resonant LC tank (series resonant frequency). The second on is the fundamental resonant frequency that is determined by all of the resonant tank components. The peak gain can be obtained from the system in the resonant frequency between series resonant frequency and fundamental resonant frequency. One of the advantages of the LLC converter is that we can get ZVS even with the light load while the converter works like a PLR and during the heavy loads it acts like a SLR. The LLC resonant converter performs like a SLR in switching frequency above resonant frequency in CCM. Therefore, the resonant converter can achieve ZVS and ZCS and decrease the switching losses.

3.5 LLC Resonant Converter for Wireless EV charger

The LLC converter is an attractive choice for the design of the wireless EV battery charger because of its high power rating, high efficiency, low electromagnetic interference emission and a wide operation range. These features are aligned with the needs of the wireless EV charger.

As it was discussed before, series loaded resonant (SLR) circuit is selected as the resonant configuration of our design. If the load resistance is transferred to the HF side of the diode rectifier and then to the primary of the transformer, the equivalent circuit of the system (Figure 3-6) could be shown with a voltage source, the resonant tank and the transferred load [25].

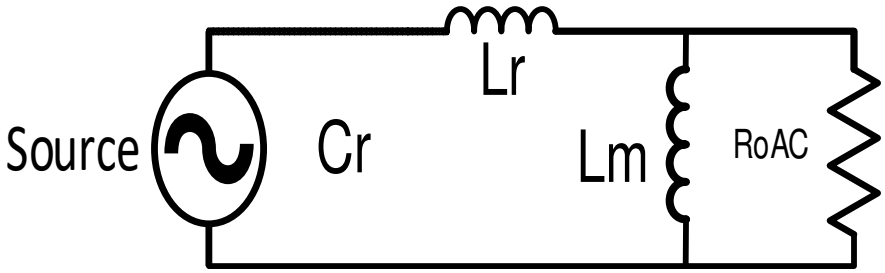

Figure 3-6. The equivalent circuit of the resonant tank

The gain of the resonant tank circuit in the Figure 4-8 is defined as the ratio between V output over R_{AC} and V source, the gain could be calculated using the following equation.

$$Gain = \frac{\frac{j\omega L_m R_{AC}}{j\omega L_m + R_{AC}}}{\frac{j\omega L_m R_{AC}}{j\omega L_m + R_{AC}} + j\omega L_r + \frac{1}{j\omega C_r}} \quad (3\text{-}1)$$

$$Gain = \frac{(j\omega L_m R_{AC}) * j\omega C_r}{(j\omega L_m R_{AC} - \omega^2 L_m L_r + j\omega L_r R_{AC}) * j\omega C_r + j\omega L_m + R_{AC}} \quad (3\text{-}2)$$

$$Gain = \frac{2\pi^2 {f_s}^2 L_m C_r R_{AC}}{2\pi^2 {f_s}^2 L_m C_r R_{AC} + j\omega L_m (\frac{f_s}{f_{r1}})^2 + R_{AC}\left(\frac{f_s}{f_{r1}}\right) - j\omega L_m - R_{AC}} \quad (3\text{-}3)$$

Assuming:

Normalized switching frequency is $f_n = \frac{f_s}{f_{r1}}$:

$$Gain = \frac{\frac{L_m}{L_r}(f_n)^2}{\frac{L_m}{L_r}(f_n)^2 + j\omega\frac{L_m}{R_{AC}}(f_n)^2 + {f_n}^2 - j\omega\frac{L_m}{R_{AC}} - 1} \quad (3\text{-}4)$$

Then considering Quality Factor as: $Q = \frac{\sqrt{\frac{L_r}{C_r}}}{R_{AC}}$

The gain is defined as:

$$Gain = \frac{\frac{L_m}{L_r}(f_n)^2}{\frac{L_m}{L_r}(f_n)^2 + {f_n}^2 - 1 + j({f_n}^3 - f_n)Q\frac{L_m}{L_r}} \quad (3\text{-}5)$$

While:

Reflected load resistance to the AC side equals to (3-6).

$$R_{AC} = \frac{8}{\pi^2}\frac{{N_p}^2}{{N_s}^2}R_o \quad (3\text{-}6)$$

And resonant frequency f_{r1} is calculated using (3-7)

$$f_r = \frac{1}{2\pi\sqrt{L_r C_r}} \quad (3\text{-}7)$$

The gain equation is plotted in Figure 3-9 for different values of f_n and Q factor. In this figure $f_{r1}$is the first resonant frequency which is calculated using only L_r andC_r. Then f_{r2} is the calculated resonant frequency considering the whole inductance in the circuit (including the magnetizing inductance). The resonant frequencies are related to the design of the components of the system and they are fixed for all variables. However, changing the load which results in variable Q factors affects the peak value of the curve at f_{r2}.

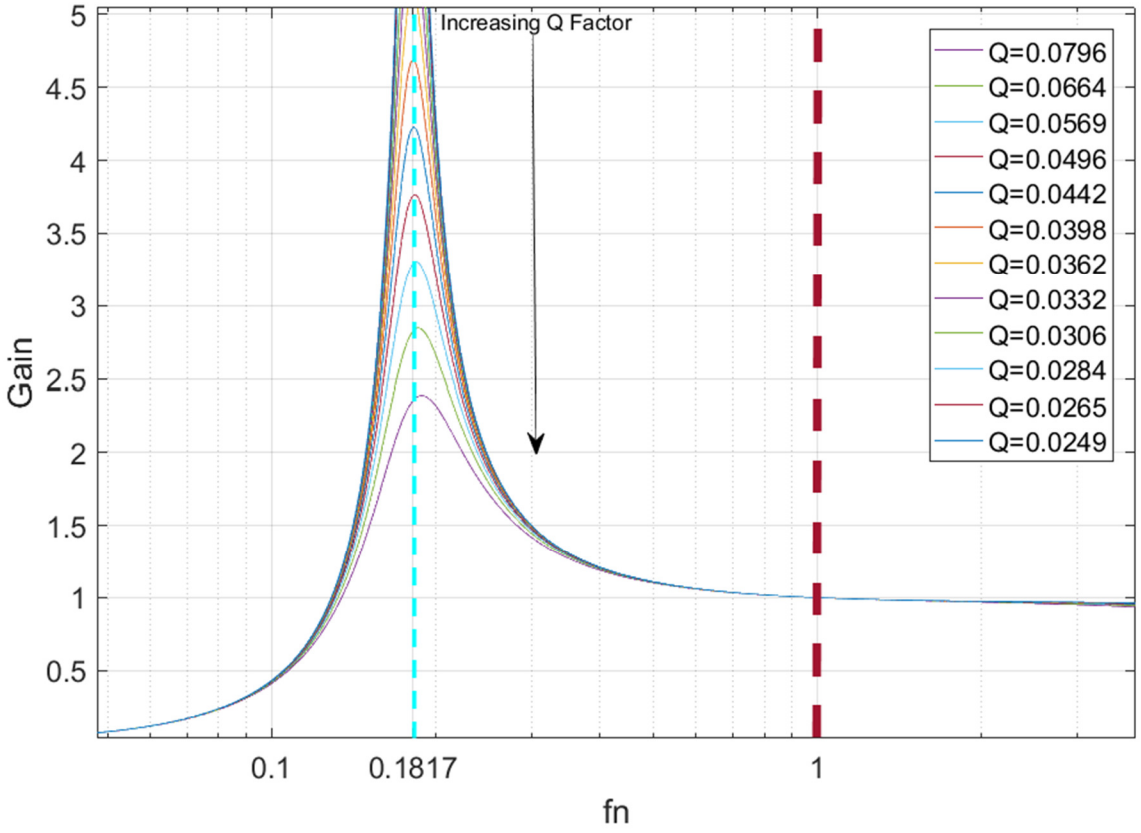

Figure 3-7. Gain vs normalized frequency of the resonant tank based on different Q.

When the load goes up, the curves will be higher and light loads results in having lower Q curves. However the curves for all of the Q factors cross the resonant frequency line at $f_{normalized}$= 1 or f_s=f_{r1} and will have a unit gain. The peak of each curve is representing the boundary between

capacitive and inductive region. Keeping the operation in the inductive region, ZVS mode of operation is achievable, since it only happens in the inductive region [26].

As it is shown in the Q curves, lighter loads and small Q values result in having higher gain in the system. Even though the curves are not sensitive to the frequency range and work in the switching frequency range higher than the resonant frequency, smaller Q values can cause more switching loss. On the other hand, heavier load and larger Q values can cause a lower gain, and a lower loss. As a result of these design trade of, the Q value should be selected appropriately for achieving an optimal point of the converter gain and high frequency efficiency. In our design Q =0.55 is selected for to calculate the parameters of resonant tank. Another parameter that is important for the design of the resonant circuit parameters is m value. We can calculate m value using equation 3-8.

$$m = \frac{L_r + L_m}{L_r} \tag{3-8}$$

Generally, the m value is selected between 3-10. Lower m values enable reaching to the higher boost gain, and more room for control and voltage regulation. However, low values of m cause having a small magnetizing inductance and higher circulating energy and conduction loss. In the trade off between gain and magnetizing inductance, the value of m in our design is selected to be 4.

After choosing the value of m and Q factor, we can calculate the parameters of resonant tank components using equations 3-1 to 3-7 [26]. Table 3-1 summarizes the design parameters.

Table 3-1. LLC resonant components parameters

	Rating	Unit
Quality Factor(Q)	0.55	
M	4	
Maximum gain	1.2	
Minimum gain	0.8	
Magnetizing Inductance(Lm)	7.75	uH
Resonant Capacitor(Cr)	11	uF
Resonant Inductor(Lr)	2.5	uH
Minimum frequency	15	kHz
Maximum frequency	60	kHz
Resonant Frequency(fr)	30	kHz

3.6 Modes of Operation Based on Switching Cycles

As it was discussed, the configuration of the HF inverter of this study is a H-Bridge with four sets of IGBT-Diode. In the H-Bridge of Figure 3-8 Switch-Diodes number 1 and 4 are the first pair and Switch Diode number 2 and 3 are the second pair. Based on the operation of this switches and the flow of current through these components eight modes of operation are defined for this converter. Half of the modes involve the first pair and the other modes involve the second pair. Also, two modes (one from each half) are for the dead times which is a rest time between

transferring the ON gate command between the first and second pair. Figure 3-9 to 3-16 shows these modes of operation and the path of the current flow in each mode with more details.

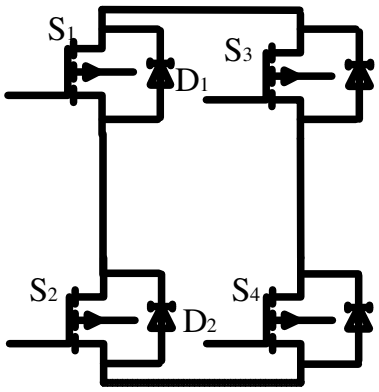

Figure 3-8. Single Phase H-Bridge inverter

The first mode starts by turning on the first pair of switches. In this mode the current flows through S_1 and S_4. This mode involves the power supply, and transformer. In this mode the current of the L_r increases [8]

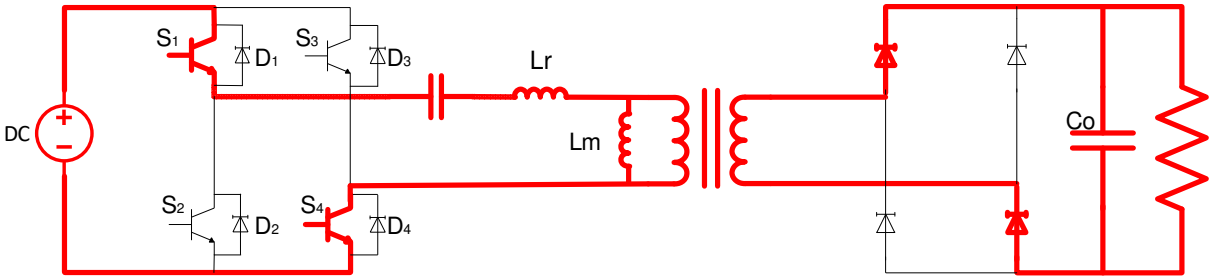

Figure 3-9. Switching mode #1

The second mode starts by turning S_4 off. The current in the Lr keeps flowing and feeding the input while it is decreasing. The return path for the current of S_1 is provided by D_3. This mode stops when the L_r current reaches the magnetizing current (the current of L_m).

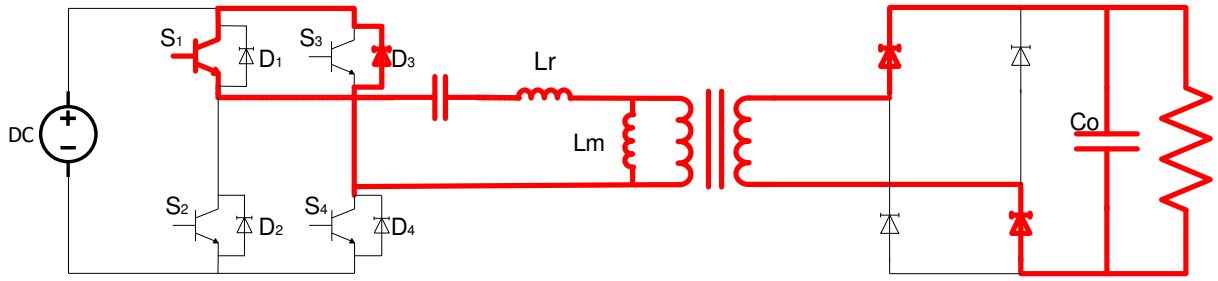

Figure 3-10. Switching mode #2

The involved switches in the third mode at the primary of the converter are similar to the second mode. However, there is no coupling between the primary and secondary of the transformer and load is fed only from the output side capacitor.

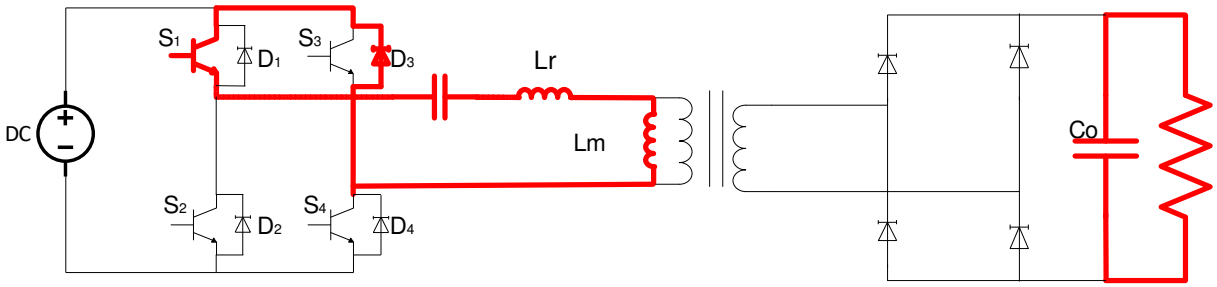

Figure 3-11. Switching mode #3

The forth mode of operation is the dead time. In this mode none of the components in the primary side of the converter is involved in the power flow path.

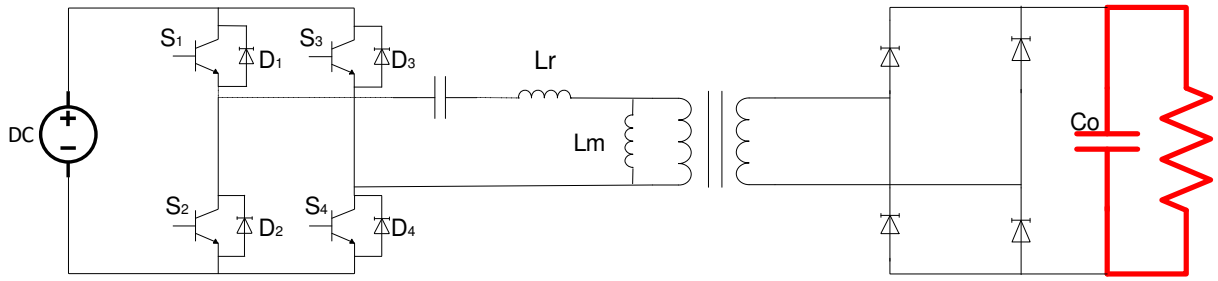

Figure 3-12. Switching mode #4

Modes #5-8 are very similar to the first four modes. The only difference is in the second half of these modes, S_2 and S_3 are the involved switches in the switching instead of S_1 and S_4.

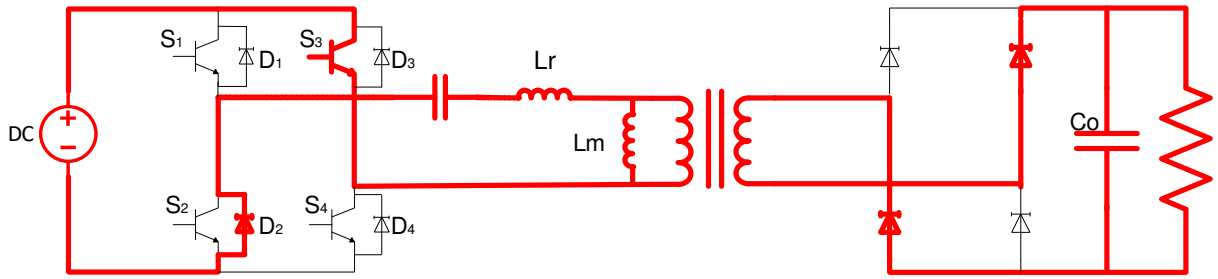

Figure 3-13. Switching mode #5

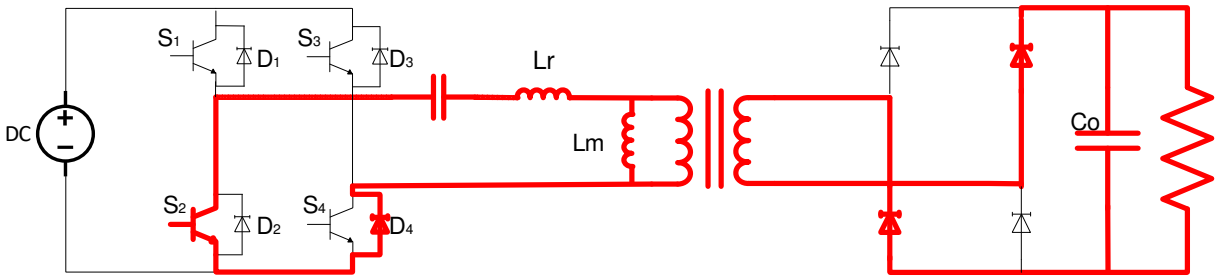

Figure 3-14. Switching mode #6

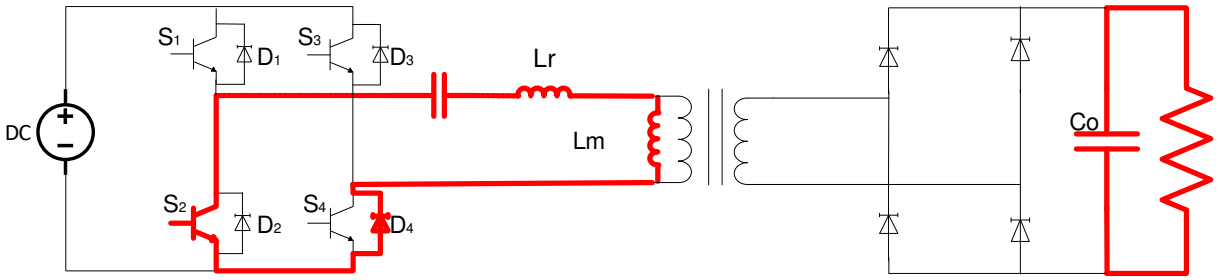

Figure 3-15. Switching mode #7

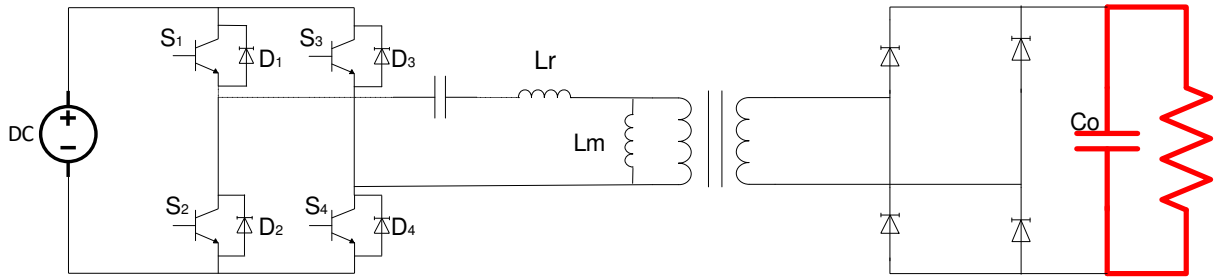

Figure 3-16. Switching mode #8

3.7 High Frequency Transformer

In order to have an efficient resonant WPT system, it is necessary to have a well design efficient transformer in the core of this system. Even though design and hardware implementation of the transformer is out of the scope of this research, the important aspects of this task are studied and discussed in this section.

Multiple factors are affecting the performance of the transformer in a WPT system. The general structure of the transformer includes two windings which are magnetically coupled through an air core. The main effective factors in the design of the transformer are distance

between the windings, leakage inductance, windings resistance and operation frequency of the system.

The total efficiency of the system depends on the Q and k factors. The efficiency of the transformer is almost inversely proportional to the distance between the two coils, so it decreases exponential by increasing the distance. However, the transformer performance is proportional to the Q (quality factor) and k (coupling factor) of the transformer.

The quality factor is defined as the ratio of the energy stored in the inductor versus the dissipated energy in the system. This factor is proportional to the frequency of the operation. As the result, the higher the operation frequency of the system, the higher the quality factor of the transformer. On the other hand, the coupling factor which is defined based on the ratio of the mutual inductance versus the self-inductance of the windings is determined based on the hardware design and physical position of the system.

The high frequency operation of the system has some disadvantages for the system. For instance, it could potentially create EMI problems, it increases the switching loss, and it increases the transformer loss. The transformer loss increases for higher f_s due to higher reactive impedance and higher skin effect. Litz wire is a common type of wire to tackle this effect in the HF converter applications. Litz wire decreases the skin effect by subdividing the conductor to very smaller insolated conductor strands with proper shields. Each of the very tiny strands in the wire is insulated from the other strands around it. Several hundreds of the strands form a larger wire size needed for the rated current. The other option to avoid the drawback of the high frequency is to use copper tube which is preferred from the point of better thermal conductivity [20-23].

CHAPTER 4

Converter Circuitry and Control Strategy Power

It is necessary to have an accurate model of the system in order to properly control the parameters of all components of the system. A proper mathematical model of the system gives a high level idea about the whole system and helps in understanding the relationship between the system parameters for optimization and computer analysis.

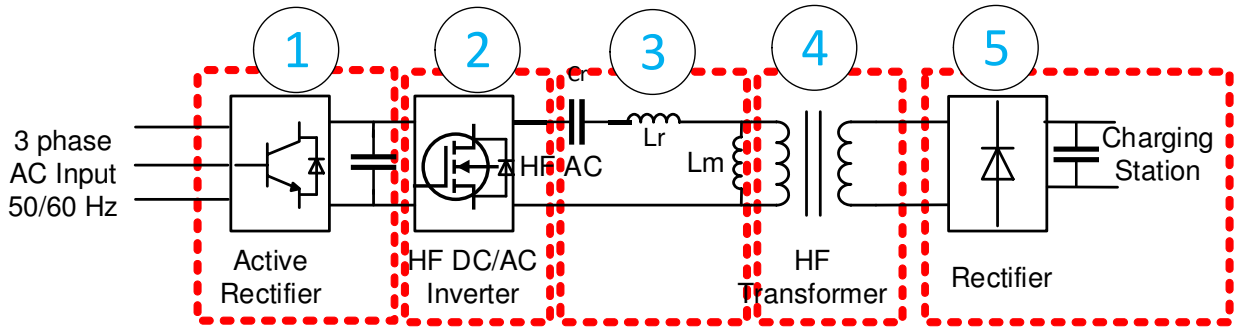

Figure 4-1. General architecture of the System components

The subject of this study includes multiple levels of power electronic converters, one resonant tank and two coupled windings. The different parts of the system are shown in this Figure 4.1. Following is the analysis of the subsystems (1) to (6).

4.1 Part 1

This first subsystem is the input three phase active rectifier. The defined task of this part is to convert the low frequency three phase input to a DC voltage. In this design the rectifier is bi-directional to potentially be able to participate in supporting the grid. This PWM rectifier is

controlled using a conventional control method which is based on transferring measured values from ABC frame to direct-quadrature-zero (dq0) synchronous rotating coordinate frame [27].

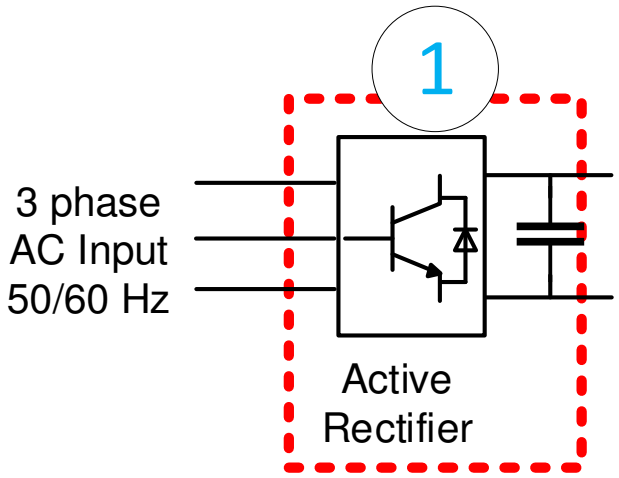

Figure 4-2, 1st Part of the Circuit-3Ph Active rectifier

In this method, three phases of the AC waveforms are transferred to dq coordinate system which is synchronous with the fundamental grid. A PLL captures the phase of the grid to be used in the control logic of the coordinate system.

Equation (4-1) shows the transformation formula between ABC and dq0 frames. This conversion simplifies the calculations and control by converting the sinusoidal math into the simple math of the DC values.

$$\begin{bmatrix} i_d \\ i_q \end{bmatrix} = \begin{bmatrix} k_d \sin\theta & k_d \sin(\theta-120) & k_d \sin(\theta+120) \\ k_q \cos\theta & k_q \cos(\theta-120) & k_q \cos(\theta+120) \end{bmatrix} \begin{bmatrix} i_a \\ i_b \\ i_c \end{bmatrix} \tag{4-1}$$

Then, the transformed values are fed into a two-PI controller to regulate the expected output DC voltage. The first PI adjusts the error of the comparison of Vdc reference and Vdc measured

and generates a reference for i_d. This reference value is compared with the id and a second PI works to make it zero. On the other hand, the reference for the iq value is set to zero and a PI controller adjusts the error between this reference and iq value to zero. The output of the last PI is fed into a reverse transform block to generate values in ABC frame from the dq frame values. The output of this block is the reference for the PWM generators.

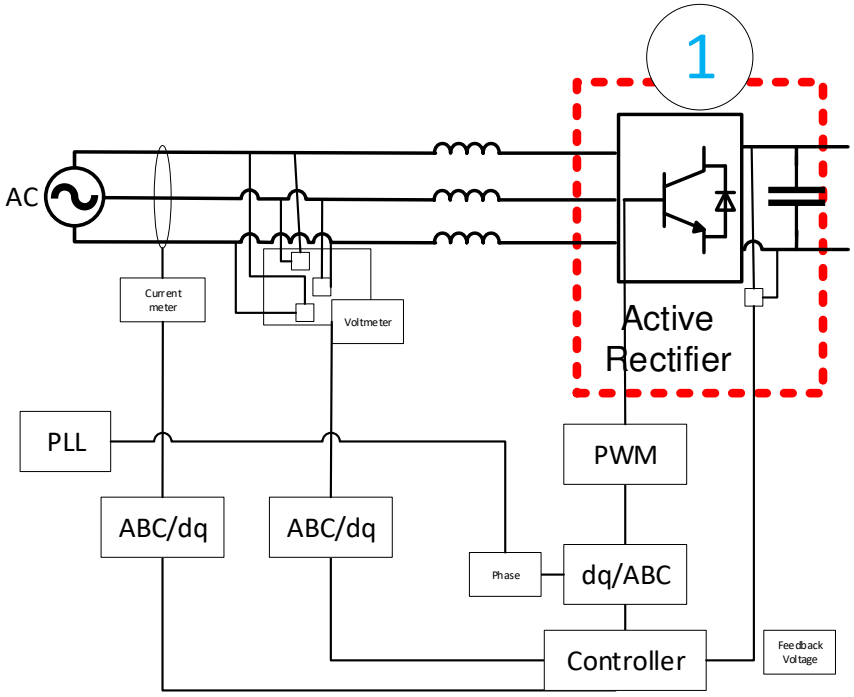

Figure 4-3. Control Structure of Three Phase Active Rectifier

The maximum DC value which could be regulated using this rectifier is equal to 1.65 times of the input AC voltage [27].

4.2 Part 2

The second part of the circuit is the HF inverter. This part converts the input side DC voltage to HF AC voltage to be fed to the resonant circuit and the transformer. The main part of the circuitry of this converter starts from this HF inverter, and finishes at the end of part 5. The main

focus of this study is on analyzing and control of this core section. The applied logic in the controller design of this section regulates the expected DC voltage at the output of part 5.

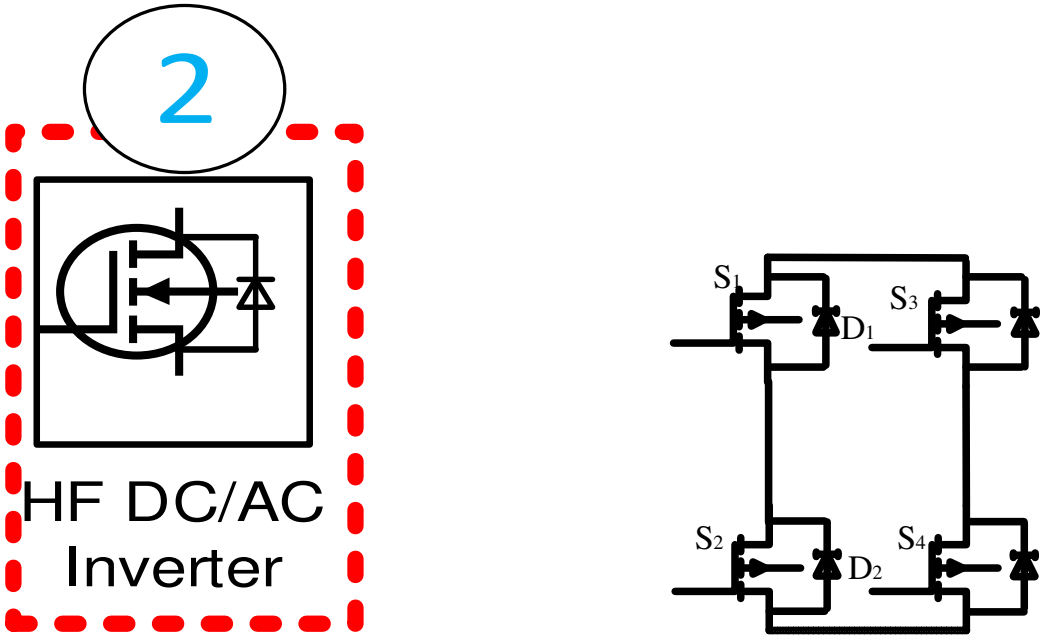

Figure 4-4. Input Side HF Inverter

The configuration of this converter is a four switch H-Bridge inverter. This single-phase converter consists of two legs. The cross switches of the two legs are paired in switching to generate a controlled AC shape waveform. The operation frequency of this converter is selected based on the design of the resonant circuit. The resonant circuitry and the gain analysis of the system based on the effect of the different parameters and variable frequencies are described in the next section.

The inverter controller uses a combination of phase shift control (PSC) and pulse frequency modulation to regulate the HF AC voltage at the output of the H-Bridge and ultimately the converter output.

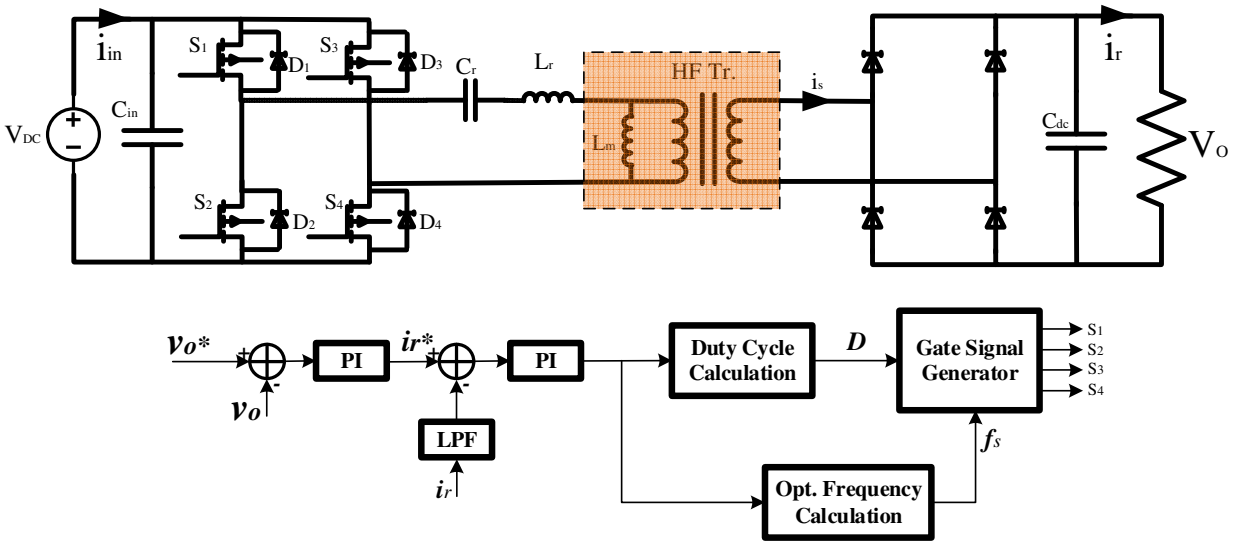

Figure 4-5. Feedback and controller configuration of the inverter

The phase shift controller is very common in the control of the converters with the similar topology. Here, in order to control the DC-DC converter between subsystems 2 to 5, there is only one active switch based converter. To apply PSC on this converter, the relative phase of the two pairs of switches is controlled to adjust the square shape output of the inverter and ultimately the DC voltage at the output of part five. This phase adjustment changes the duty cycle of the square shape AC voltage and affects the magnitude and harmonic content of the voltage which is fed to the primary of the inverter.

The gate signals (Fig. 4-6) are four repeating square shape pulses with the frequency of switching. There are two parameters in these pulses that could be used in order to control the output of the converter. The phase shift between the paired switches which determines the duty cycle of the pulses and the operation frequency of the converter. The operation frequency is also used in the control of this system to cover a wider range of load. It also helps achieving zero voltage switching (ZVS) which is limited for the whole load range in the systems with only PSC.

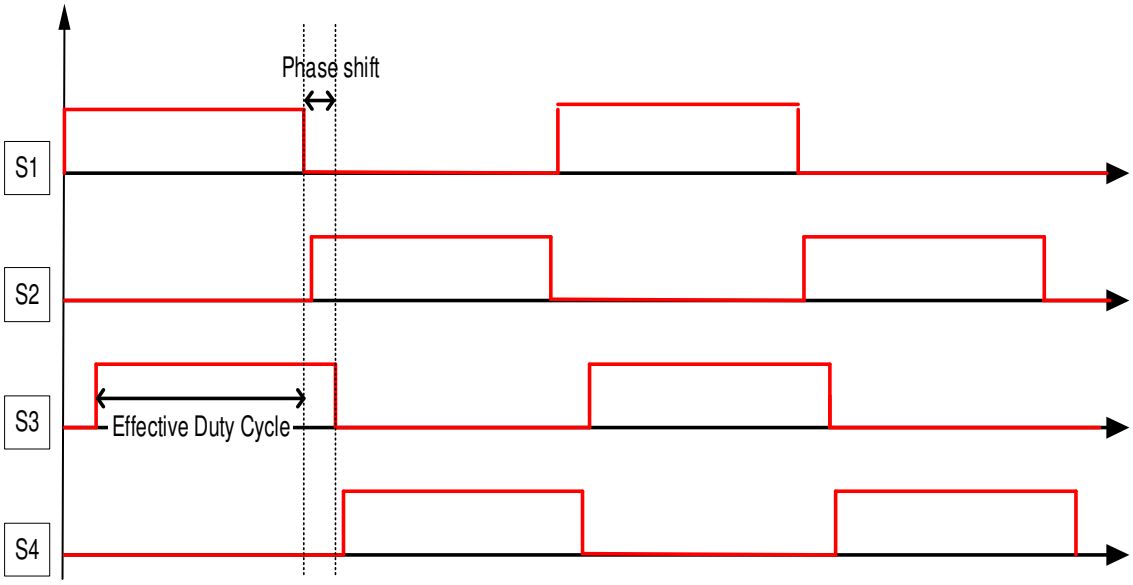

Figure 4-6. Gating of the Phase Shift Controller

4.3 Part 3

Figure (4-7) is the third part of the circuitry that is the resonant tank. The resonant thank is a passive component of the circuitry of converter. The components of this section are designed to achieve a range of resonant frequency. Type of the PE switches, magnetic design of the transformer, and expected power rating of the system are the effective parameters in the design of the resonant tank.

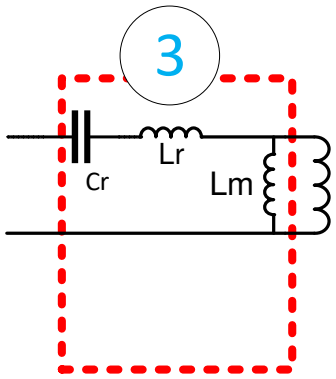

Figure 4-7. General Configuration of the Series Resonant Tank

The design of this circuit affects the controller design, operation frequency, soft switching strategy and loss and efficiency of the system. It generally consists of a capacitor and an inductor. As it was discussed before, the resonant circuitry of this converter is selected to be series loaded resonant (SLR) circuit. In this configuration one resonant capacitor (Cr), one resonant inductor (Lr), and the magnetizing inductance of the transformer form a LLC resonant system.

4.4 Part 4

The forth part of the system configuration is the transformer. In a wireless charging system, the transformer structure basically includes two windings and an air core as shown in figure (4-8).

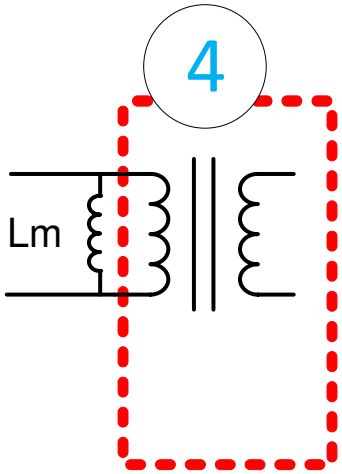

Figure 4-8 High Frequency Transformer

4.5 Part 5

Part five of this circuit is the output rectifier. This part is a diode bridge rectifier which is a passive component and does not need any direct control. The figure (4-9) shows the schematic of the output rectifier.

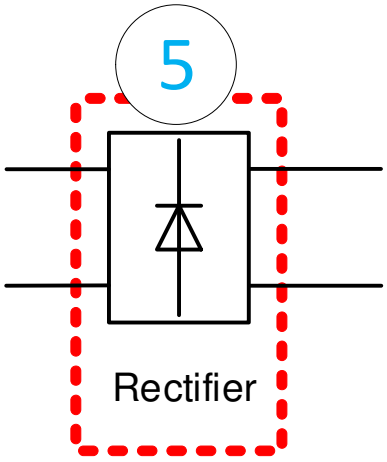

Figure 4-9 Output Side Rectifier

CHAPTER 5

Simulation and Result Analysis

5.1 Simulation of the System

The system is simulated using MATLAB/Simulink software (Figure 5-1). A 100 kW PFC rectifier is connected to the 208- 480 VAC input. It converts AC voltage to generate the input side DC voltage. The 330 kW LLC resonant dc-dc converter in the next step will regulate and control the output DC voltage for charging the car battery. The nominal power, output voltage, and maximum current of the converter are considered to be 330kW, 350V, and 950 A, respectively. The simulation is performed for different load conditions and switching frequency of 30 kHz. Table 5-1 shows the parameters that are used in the simulation.

Table 5-1.simulation parameters

Item	Rating	Unit
Input voltage	600-800	V
Output Voltage	350	V
Output Power	330	kW
Maximum Current	950	A
Resonant Frequency(fr)	30	kHz
Minimum Frequency(f2)	15	kHz
Maximum Frequency(f1)	60	kHz

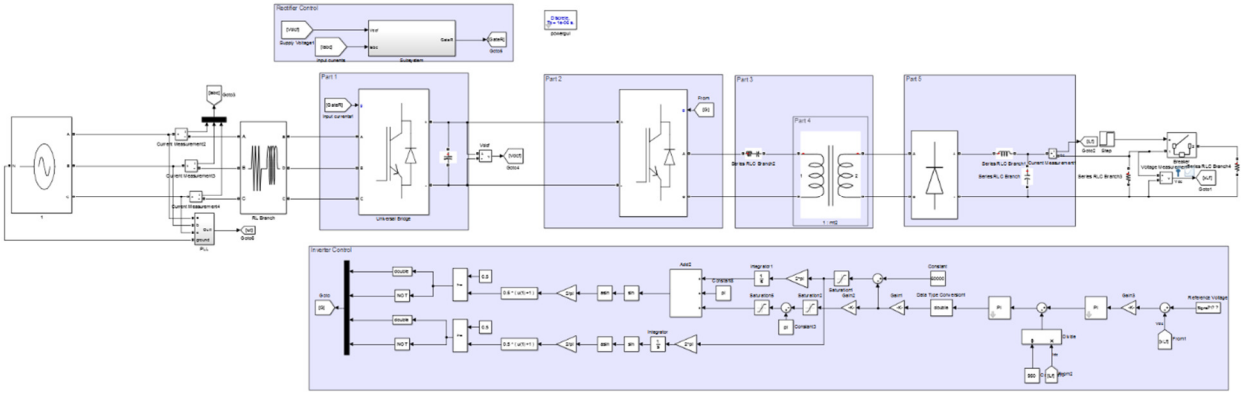

Figure 5-1. Simulated circuit in MATLAB/Simulink environment

5.2 Output Voltage, Current, and Power for Different Loads

A controller using a combination of frequency control and phase shift control is developed and used for this system, in order to adjust current and regulate the output voltage of the system. Figure 5-2 shows the output voltage, current, and power waveforms for the system in the different conditions. It also shows how the controller regulates the reference values. Frequency and phase shift controller are a working together to meet the requirements. Each scope is divided into three parts, in order to simplify the explanation of the details which will be discussed in the following sections. The frequency and phase shift changes for meeting the target voltage and power is shown in 5-3.

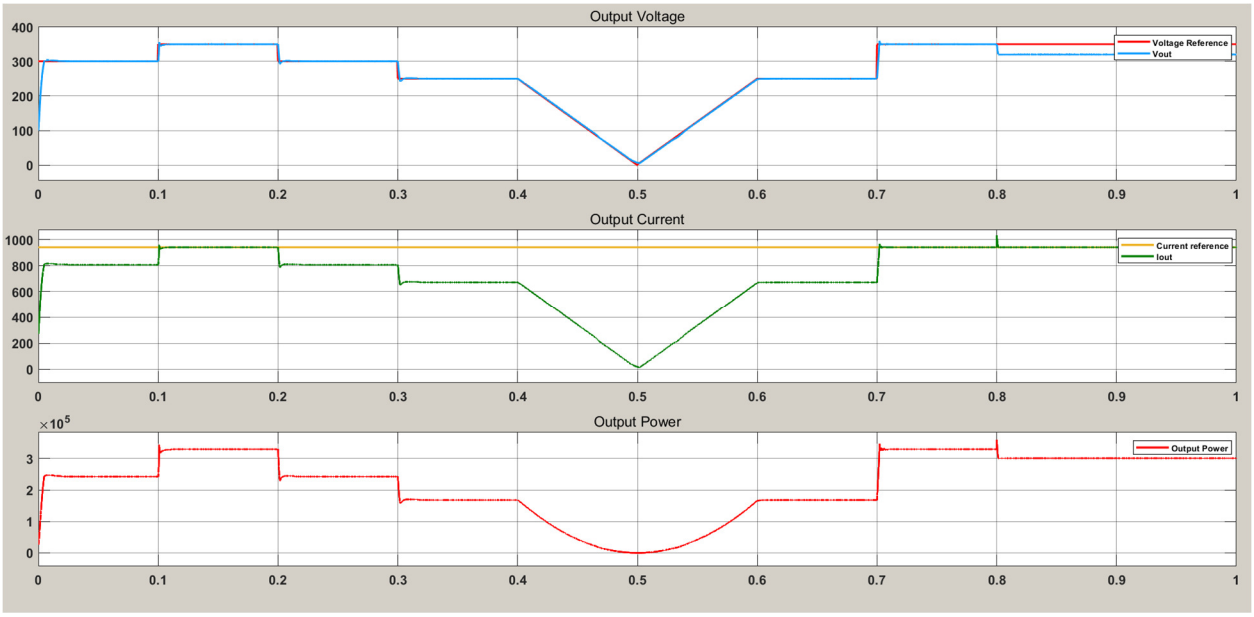

Figure 5-2. Waveforms of output voltage, current and power between 0-1second.

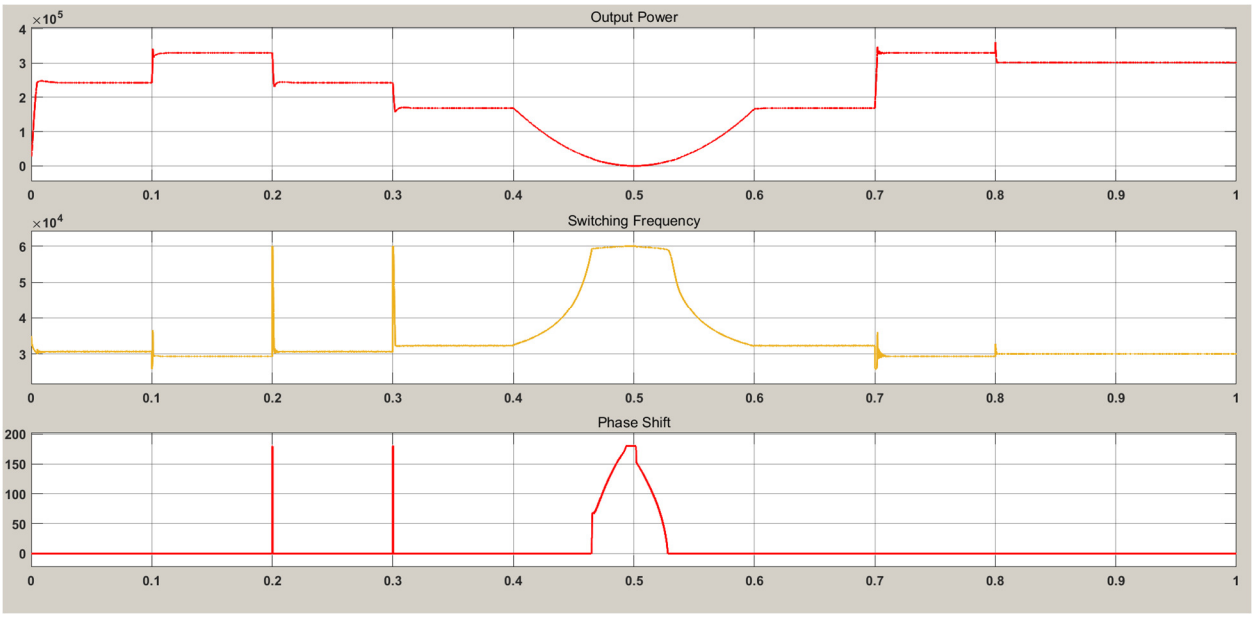

Figure 5-3.Waveforms of output power, switching frequency and phase shift between 0-1 s.

The waveforms in figure 5-4 show the output voltage, current and power of the system between the time 0-0.3 second. The voltage reference for the output voltage is the red color waveform in the first scope which starts from 300V with the upper limit of 350V. The blue waveform, is the actual output voltage which starts from zero and goes up to 300V in the first step. It stays constant until the reference voltage changes to 350V at 0.1 second. The second change will happen for the system at 0.2 second. The simulation results show that the system can properly regulate the output voltage based on the reference values. However, the reference current which is set as the maximum current limit is constant and equal to 950A during this time interval.

The output current waveform starts from zero and increases to 800A until the time 0.1 second, and then increases to 950A by increasing the output voltage. The output power of the system is shown with the red color in figure 5-4. The output power changes as the result of the changes in the current and voltage levels. Power of the system will reach its maximum peak of 330 kW between the times 0.1-0.2 second.

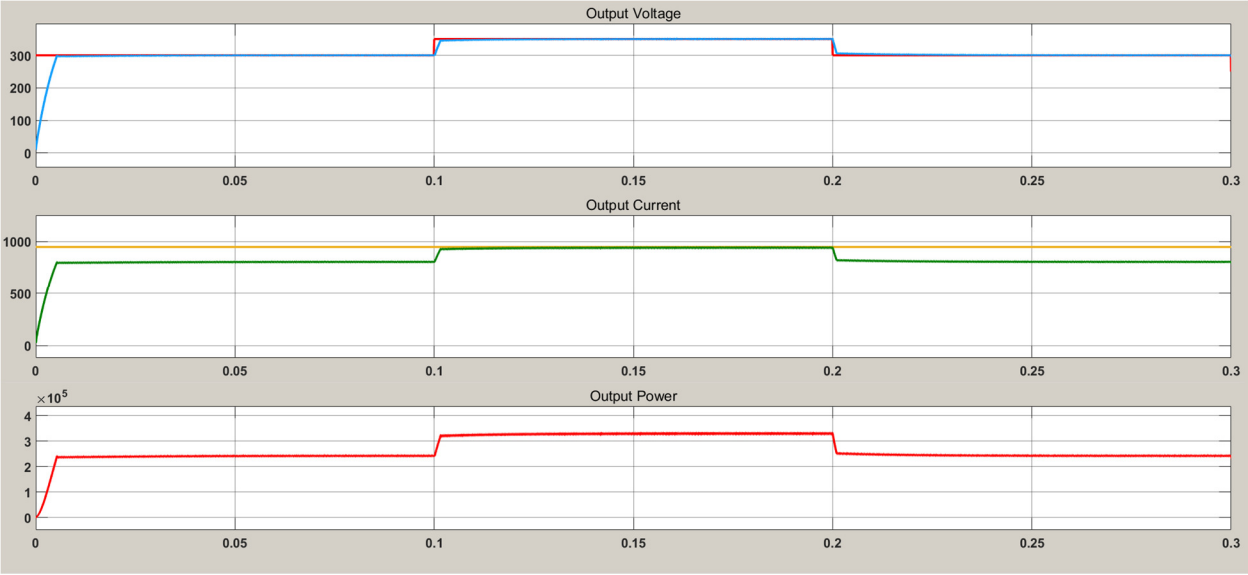

Figure 5-4. Waveforms of output voltage, output current, and output power between 0-0.3 s.

Figure 5-5 shows the changes in the switching frequency and phase shift value between the time 0-0.3 second. The output voltage in some levels could be regulated using only frequency control and there is no need for the phase shift changes. However, when the operation frequency is limited between 20 kHz to 60 kHz, the phase shift control helps the controller to meet the requirements.

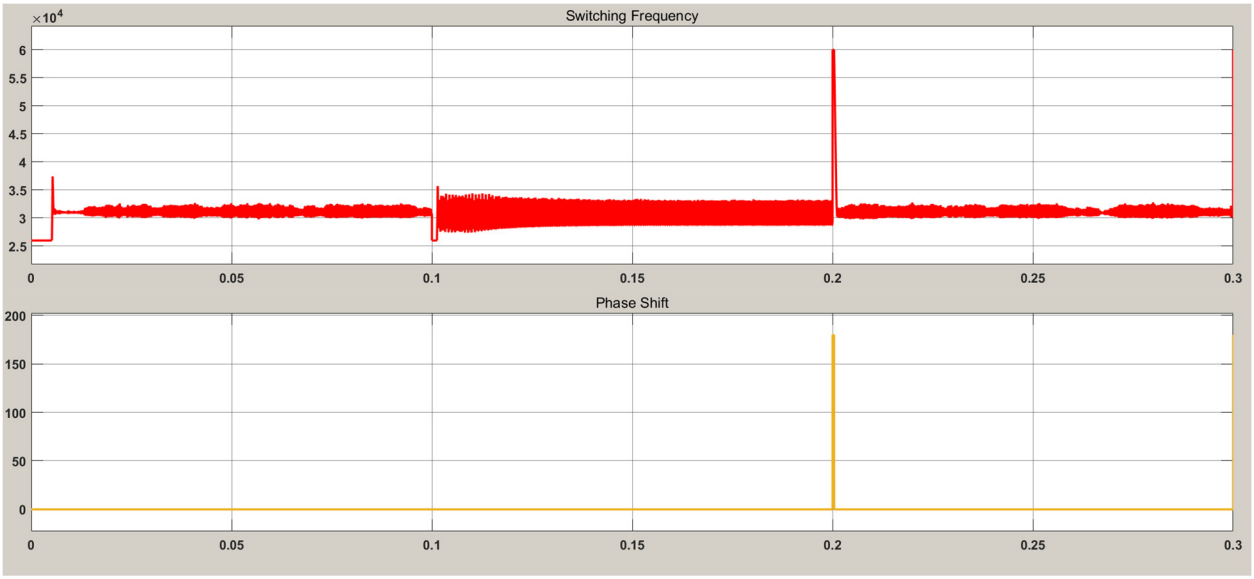

Figure 5-5. Waveforms of switching frequency and phase shif between 0-0.3 s.

Figures 5-6 and 5-7 are the simulation results of the output parameters between the of 0.3-0.7 second. The reference output voltage which is 250 is reduced close to zero between the time 0.4 -0.5 second. The output voltage could be regulated to this reference value by frequency control. However, at the time 0.44 second, frequency of the inverter is at its maximum point, and cannot go higher to reduce the output voltage more. Then, the controller's response is to increase the phase shift to decrease the effective duty cycle. This reduces the output voltage to follow the output reference. The phase shift could reach 180 degrees which is zero duty cycle and the converter is not converting any voltage at the AC side in this phase.

Then, in the time between 0.5-0.6 second, the output reference increases to the voltage of 250V again. In this situation, frequency and phase shift control are still working together until a certain value of output voltage. After that, when the frequency is in the range between upper and lower limit of the frequency for the system, frequency control can regulate the output voltage without phase shift controller.

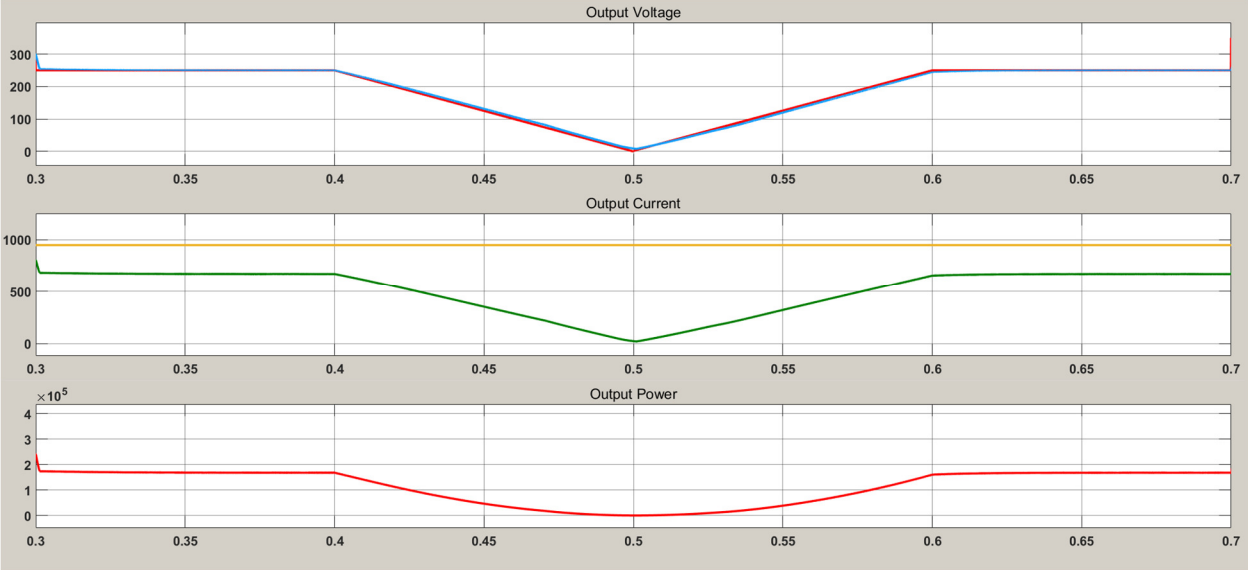

Figure 5-6. Waveforms of output voltage, output current, and output power between 0.3-0.7 s.

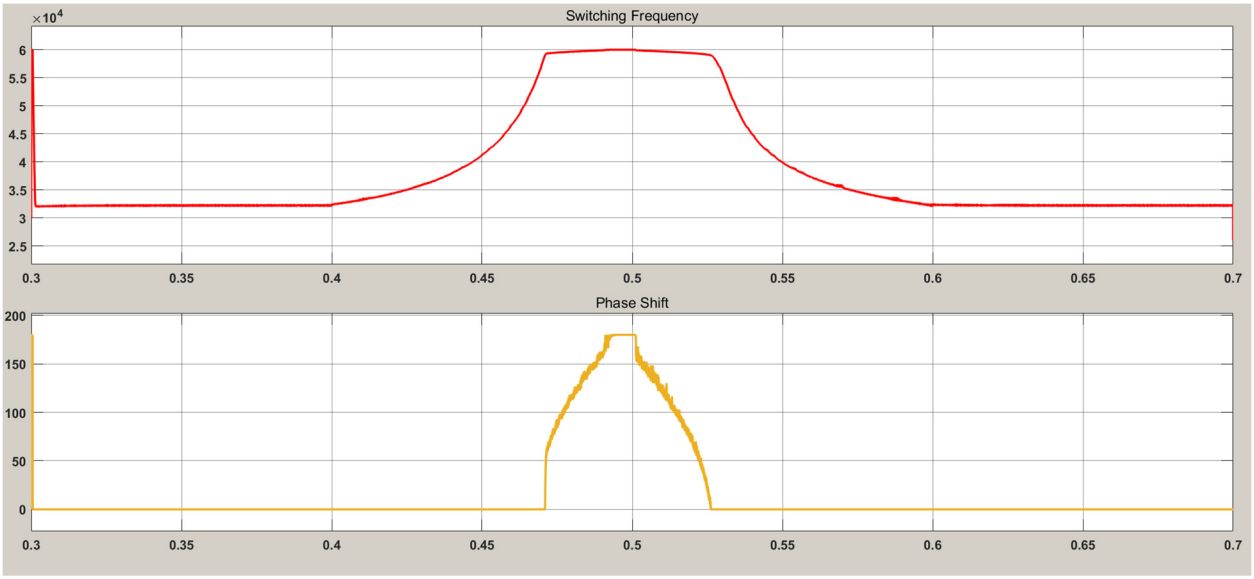

Figure 5-7. Waveforms of switching frequency and phase shif between 0.3-0.7 s.

At the time between 0.7 to 1 second, another load is increased. The effect of the load change in the system is shown in the waveforms of the figures 5-8 and 5-9. The system is working in its maximum voltage, current and power until the time 0.8 second that an extra load was added to the output. In this condition, the output current will go up arbitrary, but the current of the system was at its maximum of the 950 A. In order to prevent current from increasing higher than the desired value, the voltage decrease from its maximum while the reference voltage is still 350 V. As a result, the current stay at its peak while the voltage and the output power will decrease. The phase shift control is not working at this time, but the frequency control is working to manage the system based on the output feedbacks. Figures 5-8 and 5- are the waveforms of output parameters in the time between 0.7 and 1 second.

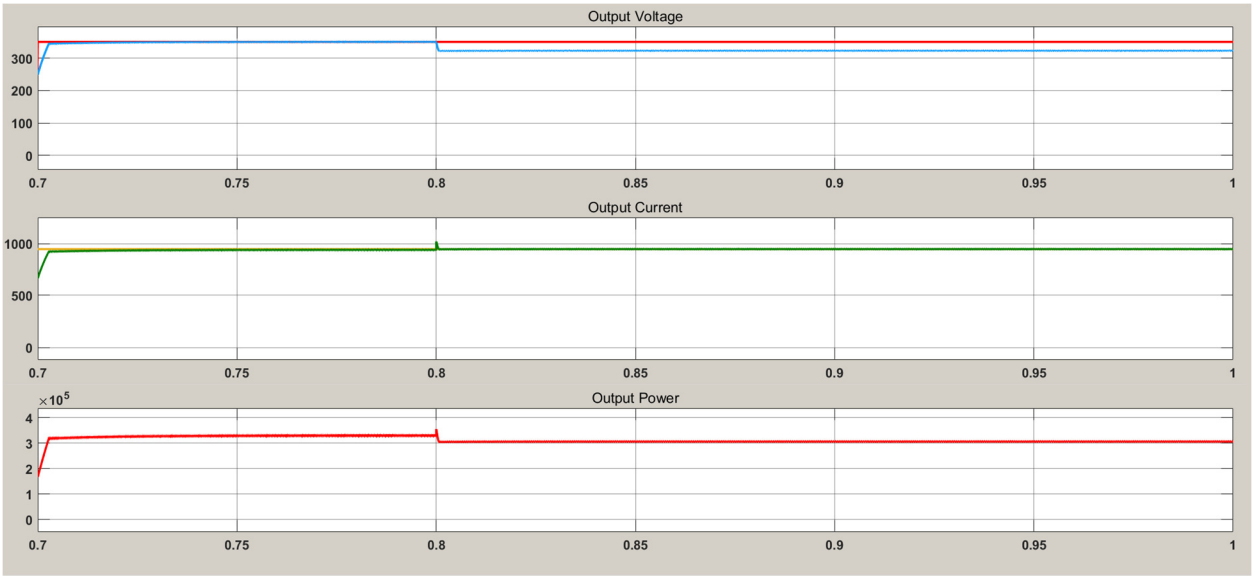

Figure 5-8. The waveforms of output voltage, current and power between 0.7-1 s.

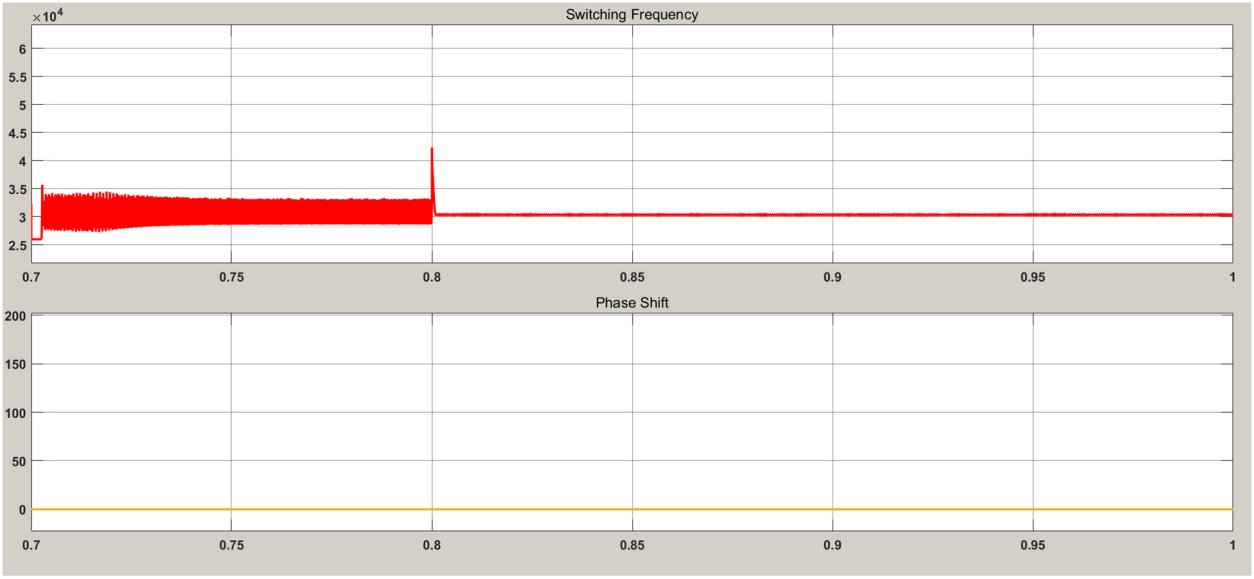

Figure 5-9. Waveforms of switchig frequency and phase shift between 0.7-1 S.

5.3 Modes of Operation

As it was explained in chapter 3, there are three modes of operation for the converter based on different loads, and input voltage conditions. The three modes of operation are below the resonance, at the resonance and above the resonance frequency.

In each of these three modes, the converter has two possible operations within the switching cycle that are power delivery operation and freewheeling operation. Each mode may include one or both of these operations.

The power delivery operation happens twice in a switching cycle; when the resonant tank is excited with the positive and negative voltages. Positive voltage causes positive direction for the current of resonant tank in the first half of the switching cycle while negative voltage causes the current to resonate in the negative direction. The negative and positive output voltage reflect on the magnetizing inductor and the magnetizing current are charged and discharged respectively. The difference between the resonant current and the magnetizing current goes to the secondary side of the transformer through the rectifier and power delivers to the load [26].

The freewheeling operation happens when the switching frequency is below the resonant frequency(fs<fr) when the magnetizing current is equal to the resonant current, and the current in the secondary side reaches zero while no power transfers to the secondary side.

The simulation results clearly show the two operations in the three modes of frequency. When the switching frequency of the converter is equal to the resonant frequency that is 30 kHz in this system, the resonant half cycle is completed during the switching half cycle and each of the half switching cycle has a complete power delivery operation [26]. The waveform in the figure 5-10 shows the input voltage, and resonant current and voltage when fs=fr.

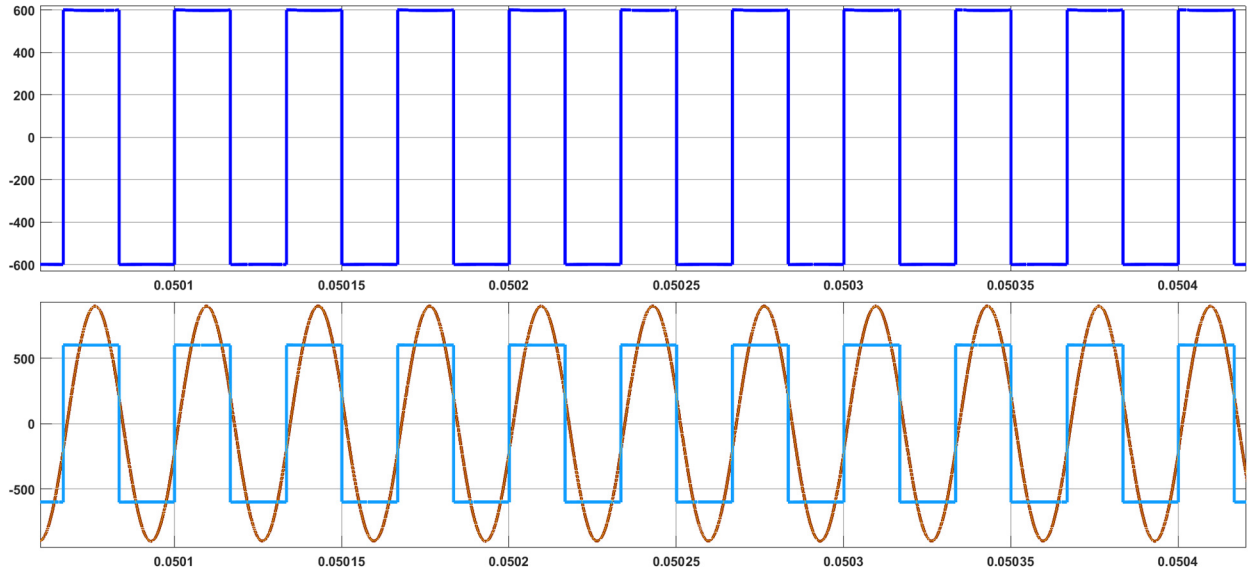

Figure 5-10. Waveforms of input voltage, inverter's current and voltage when fs=30kHZ

The input DC voltage is 600V in this frequency, and the converter operates at its nominal input and output voltages. The magnetizing current is equal to the resonant current, and the current of the secondary side reaches zero at the end of each half cycle.

The simulation results are also shown when the switching frequency is above resonant frequency that is fs>30kHz. In this case, the resonant half cycle is interrupted by the starting of the other switching half cycle. As a result, a partial power delivery happens in each switching half cycle, and the turn off loss on the primary MOSFET increases. Figure 5-11 is the waveform of the input voltage, inverter's voltage and current in this mode.

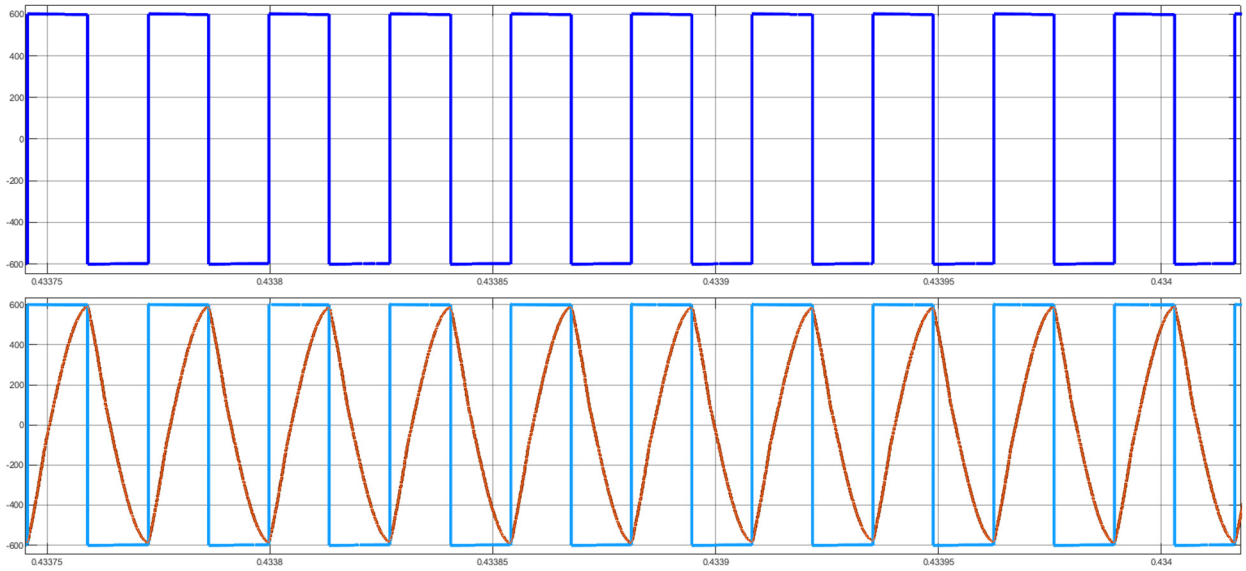

Figure 5-11. Waveform of input voltage, inverter's current and voltage when fs> 30kHZ

The maximum switching frequency of the converter is 60kHZ. the waveform in the figure 5-12 shows the waveform of input voltage, inverter's voltage and current in this frequency.

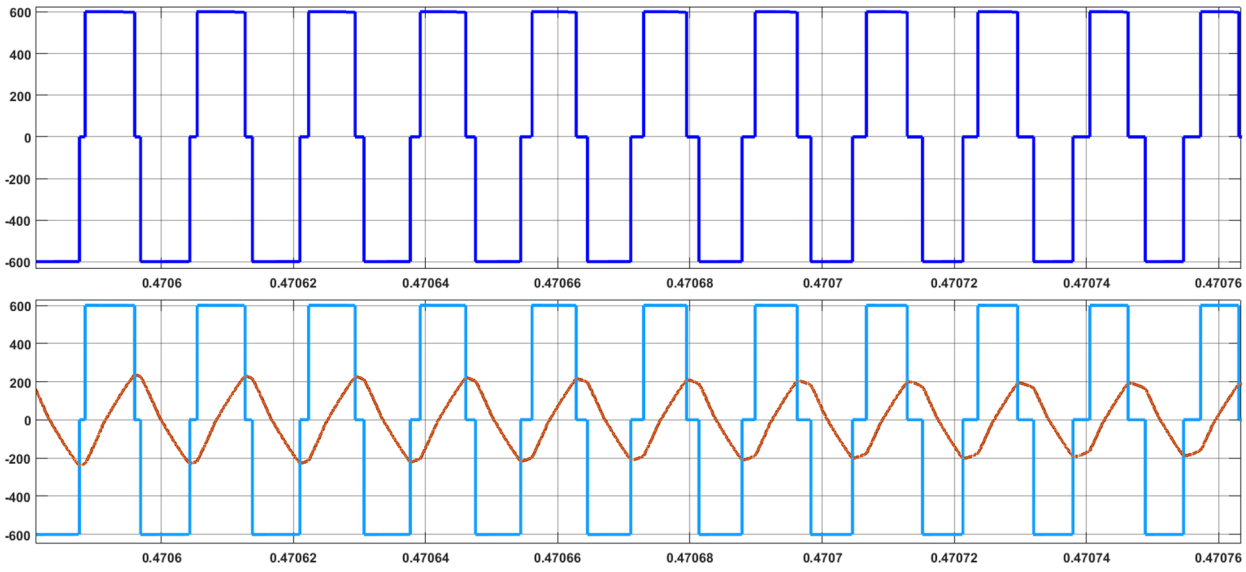

Figure 5-12. The waveforms of input voltage, resonant voltage and current when fs=60kHz

The third mode of operation in this system happens when the switching frequency is below the resonant frequency, fs<30kHZ. In this mode we have both power delivery operation and freewheeling operation in each switching half cycle. When the power delivery is completed in the first resonant half cycle, and magnetizing current reaches to the resonant current, the rectifier's current decreases to zero, and the freewheeling operation starts until to the end of switching half cycle. The resonant current changes slightly in the freewheeling interval. Figure 5-13 shows the waveforms of input current, inverter's voltage and current when fs<30 kHz.

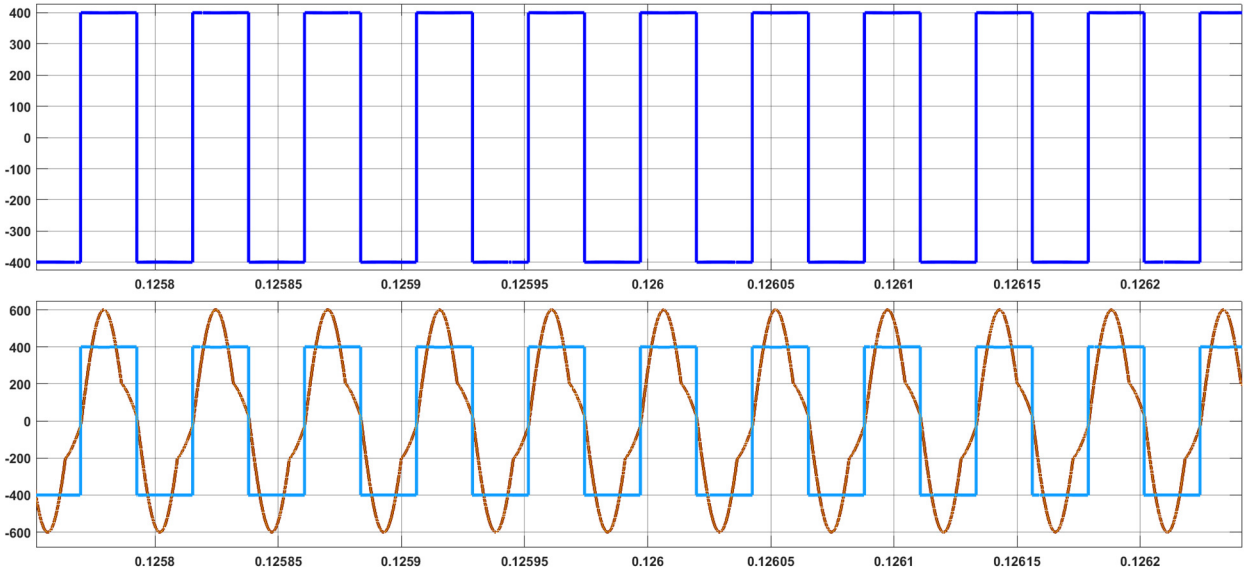

Figure 5-13.Waveforms of input voltage and inverter's voltage and current when fs<fr

5.4 Efficiency

The energy efficiency of the wireless charger system depends on the loss in the different components of the system. This includes the efficiency and loss in three phase rectifier, and LLC resonant converter (switching loss, and the transformer loss).

The converter is designed based on the wideband gap devices. The preferred PE switch for the selected range of frequency is SiC based MOSFET and diodes. Diode conduction has a significant loss relatively, In the industrial applications, choosing a low loss diode can improve the efficiency of the system. for the diode bridge rectifier part, the efficiency is the ratio of the output DC power to the total amount of AC power from the transformer.

The expected efficiency of this topology based on the illustrated design and component selection is shown in the following table. Based on the literate review and simulation results the efficiency of this system is around 95%.

Table 5-2. Itemized efficiency of the system

Item	**Part description**	**Efficiency %**
Part#1	Three phase grid connected active rectifier	95
Part#2	HF single phase H-Bridge inverter based on SiC Mosfet	98
Part#3	Single Phase Diode Bridge Rectifier	96
Part#4	Transformer	99
Total	The whole system	95

5.5 Power Loss Calculation

An approximation of power loss of the system can be calculated by finding three major components of the loss that are wiring loss (Pw), switching loss of the system(Ps), and core loss of the transformer (Pc). These parameters can be found by using the equations (5-1) -(5-7). Wiring loss is the combination of the loss of MOSFETs, the copper loss of the transformer, and the

conduction loss of the diodes. Power loss of the system is the summation of all the major loss components. Rt in the equation (5-2) is the resistance on the MOSFETs, diodes, and the transformer wires altogether. In order to find the switch loss, a CREE MOSFET is chosen for this application and a second order polynomial is fitted over E_{ON} and E_{OFF}. The ON+OFF energy is multiplied by the switching frequency.

Resonant current of the system, and output power of the system also can be calculated by using equations (5-6), and (5-7).

$$P_{loss} = P_w + P_s + P_c \tag{5-1}$$

$$P_w = R_t I_r^2 \tag{5-2}$$

$$P_s = (aI_r^2 + bI_r + c) f_{sw} \tag{5-3}$$

$$P_c = k_c f_{sw}^{\alpha} B^{\beta} \tag{5-4}$$

$$B = \frac{\frac{4V_i}{\pi}\sin(\frac{\pi-\varphi}{2})}{2\pi f_{sw} A} \tag{5-5}$$

$$I_r = |\frac{4}{\pi} V_i \sin(\frac{\pi-\varphi}{2}) \frac{1}{\frac{j\omega_s L_r + 1}{j\omega_s C_r} + \frac{j\omega_s L_m R_e}{j\omega_s L_m + Re}}| \tag{5-6}$$

$$P_{out} = \frac{V_o^2}{R_e} = \frac{V_i^2 M^2}{R_e} \tag{5-7}$$

The core loss of the transformer is related to the switching frequency, f_{sw}, and the flux density, B. A ferrite core is chosen, and the coefficients of the loss function are fitted based on the data sheet.

The charger's power can be controlled by the phase shift (duty cycle) or the switching frequency (gain , M). The power regulation approach in this project is as follow:

When the power is low, the switching frequency is kept constant at 60 kHz and the power is regulated by adjusting the phase shift.

However, for higher power when the duty cycle is saturated, the power is being regulated by adjusting the switching frequency. Lower switching frequency corresponds to higher gain which increases the power transfer. Waveforms of the calculated loss, and efficiency of the system are shown in figures (5-14)- (5-16).

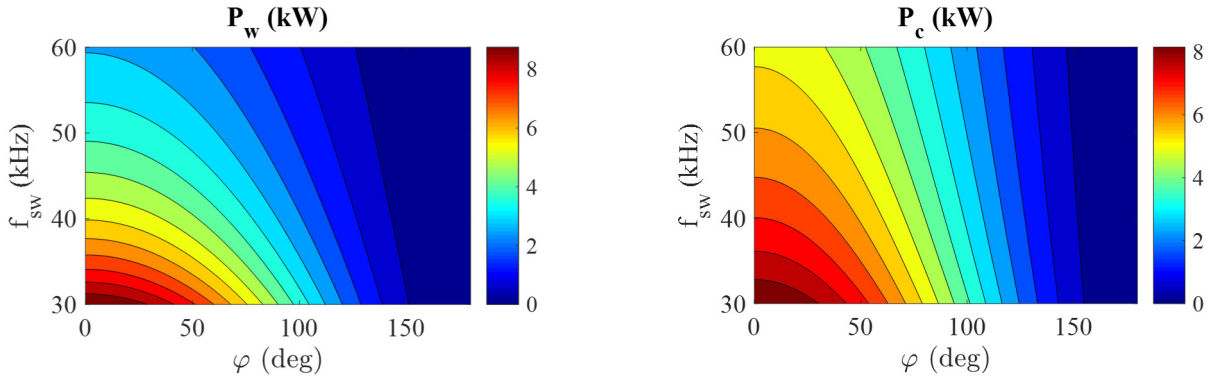

(a) (b)

Figure 5-14. Different loss parameters: (a) Wiring loss, (b) core loss of the transformer.

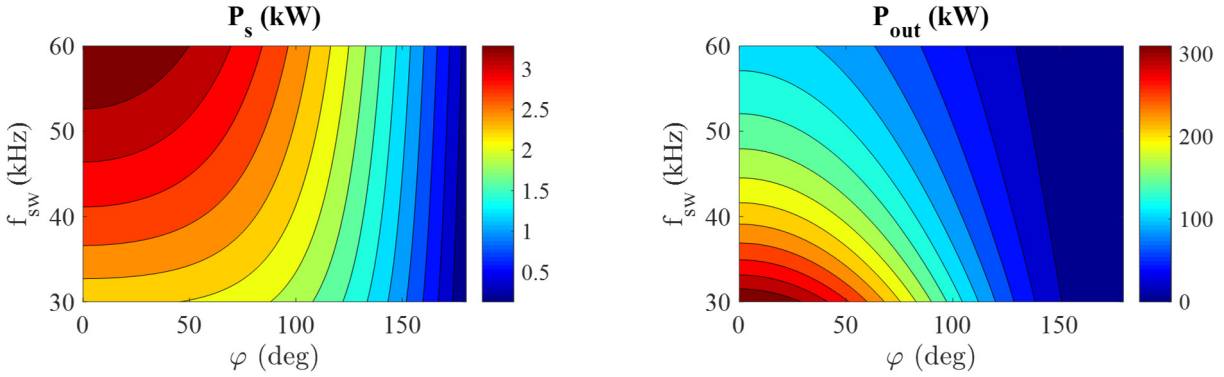

(a) (b)

Figure 5-15. Different power components: (a) Switching loss, (b) Output power.

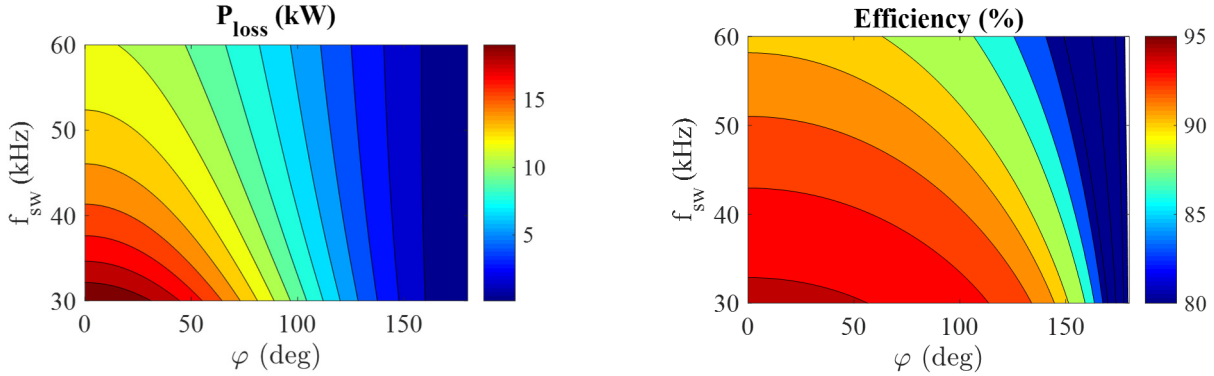

(a) (b)

Figure 5-16 . Total power parameters: (a) Total loss of the system, (b) Efficiency of the system

The wiring loss always has the same pattern as output power in this system and is at its maximum when fsw = 30kHz. Navy blue color in the waveforms is the minimum power, and dark red shows the maximum power. Core loss of the system also will be higher at this frequency which is the resonant frequency of the converter as shown in the figure 5-14. (b). However, switching loss of the system will be higher at the maximum switching frequency of the system which is 60 kHz. When the three loss parameter of the system are calculated, the total power loss of the system can be found easily. As shown in figure 5-15. (b), the maximum output power of the system can be

achieved when the switching frequency is equal to resonant frequency of the system, and also power loss of the system will be at its maximum in this point. As a result, the maximum efficiency of the system will be achieved when the system is working at its resonant frequency.

CHAPTER 6

Conclusion

The focus of this research is on modeling, analyzing, and simulation of a resonant topology for Wireless Power Transfer for the application of charging electrical vehicles. Development of this technology is attracting a lot of attentions in the car industry to provide safer and more convenience charging experience for the EV car drivers. In addition, with the increasing number of EVs, the WPT chargers enables some other features like charging while the car is moving, and charge share between vehicles in the near future.

The latest technology developments in the field of power electronics, which allow compact design of the high power and high frequency design of the power electronics converters, is a major enabler factor for this technology.

The illustrated topology of this research is a grid connected charging station with an integrated energy storage on the primary side converter for supporting the high demand in the peak time periods. This energy storage station is sized as one third of the nominal power of the power electronic stations after it. It is also defined with the capability of supporting the grid in the event of the demand for active or reactive power.

Different components of the converter are illustrated, and mathematically analyzed in this research. It starts with a grid tied three-phase active rectifier. The control and simulation of this topology is described based the classic method of converting the signals from the ABC frame to the dq0 frame. However, the main focus of the design and control development in this work is on

parts after the input side DC busbar. This section of the circuitry includes a HF inverter, a resonant tank, a HF transformer and a HF diode bridge rectifier.

The resonant design of the converter helps achieving soft switching in the converter. The configuration of the LLC resonant circuit is analyzed, mathematically modeled and simulated to help the design of the whole system. This detail analysis helps the designers in selecting optimal frequency of operation and sizing the components of the resonant tank. These factors directly affect the design of the transformer and highest achievable efficiency level for the converter.

The technologies of electrical cars, hybrid and hybrid plug-in cars is introduced briefly. Then the different known topologies of WPT technologies are categorized, introduced and illustrated in this study.

A mix of phase shift and variable control method is selected to control the flow of current and regulate to voltage at the charging port. The controller varies the frequency between 30 kHz to 60 kHz. The modes of operation of DC/DC part of the circuit is analyzed based on the path of current through switches and diodes.

Finally, the modeled system is simulated. The simulation results show the effectiveness of the proposed design and control method for delivering a regulated voltage, and regulated level of power to the output port and to achieve soft switching. The system is evaluated with different reference command. The controller properly meets the target and achieves the soft switching which reduces the switching loss dramatically.

REFERENCES

[1] A. Ahmad, M. S. Alam and R. Chabaan, "A Comprehensive Review of Wireless Charging Technologies for Electric Vehicles," in *IEEE Transactions on Transportation Electrification*, vol. 4, no. 1, pp. 38-63, March 2018

[2] Vidyanandan, K.V. (2018). Overview of Electric and Hybrid Vehicles. Energy Scan (A House Journal of Corporate Planning, NTPC Ltd., India). III. 7-14.

[3] S. Habib, M. M. Khan, K. Hashmi, M. Ali and H. Tang, "A Comparative Study of Electric Vehicles Concerning Charging Infrastructure and Power Levels," *2017 International Conference on Frontiers of Information Technology (FIT)*, Islamabad, 2017, pp. 327-332

[4] F. Zhang, X. Zhang, M. Zhang and A. S. E. Edmonds, "Literature review of electric vehicle technology and its applications," *2016 5th International Conference on Computer Science and Network Technology (ICCSNT)*, Changchun, 2016, pp. 832-837

[5] D. H. Tran, V. B. Vu and W. Choi, "Design of a High-Efficiency Wireless Power Transfer System with Intermediate Coils for the On-Board Chargers of Electric Vehicles," in IEEE Transactions on Power Electronics, vol. 33, no. 1, pp. 175-187, Jan. 2018.

[6] A. Caillierez, D. Sadarnac, A. Jaafari, A. Caillierez and S. Loudot, "Unlimited range for electric vehicles," 2014 International Symposium on Power Electronics, Electrical Drives, Automation and Motion, Ischia, 2014, pp. 941-946.

[7] H. Zeng and F. Z. Peng, "SiC-Based Z-Source Resonant Converter with Constant Frequency and Load Regulation for EV Wireless Charger," in IEEE Transactions on Power Electronics, vol. 32, no. 11, pp. 8813-8822, Nov. 2017.

[8] Y. Iga, H. Omori, T. Morizane, N. Kimura, Y. Nakamura and M. Nakaoka, "New IPT-wireless EV charger using single-ended quasi-resonant converter with power factor correction," 2012 International Conference on Renewable Energy Research and Applications (ICRERA), Nagasaki, 2012, pp. 1-6.

[9] A. Ahmad, M. S. Alam and R. Chabaan, "A Comprehensive Review of Wireless Charging Technologies for Electric Vehicles," in IEEE Transactions on Transportation Electrification, vol. 4, no. 1, pp. 38-63, March 2018

[10] Chirag Panchal, Sascha Stegen, Junwei Lu,"Review of static and dynamic wireless electric vehicle charging system" Engineering Science and Technology, an International Journal,Volume 21, Issue 5,2018, Pages 922-937,ISSN 2215-0986

[11] Rahman, F.K.A. & Saat, Shakir & Yusop, Yusmarnita & Husin, Huzaimah & Yahya, Aziz. (2017). Design and Analysis of Capacitive Power Transfer System with and without the Impedance Matching Circuit. International Journal of Power Electronics and Drive Systems (IJPEDS). 8. 1260. 10.11591/ijpeds. v8. i3.pp1260-1273.

[12] J. Garnica, R. A. Chinga and J. Lin, "Wireless Power Transmission: From Far Field to Near Field," in Proceedings of the IEEE, vol. 101, no. 6, pp. 1321-1331, June 2013.

[13] H. H. Wu, A. Gilchrist, K. Sealy, P. Israelsen and J. Muhs, "A review on inductive charging for electric vehicles," *2011 IEEE International Electric Machines & Drives Conference (IEMDC)*, Niagara Falls, ON, 2011, pp. 143-147

[14] Tarakci, Sedat & Bilic, Gokay & Karabulut, Abtulgalip & Ozdemir, Serhan. (2018). Demands in Wireless Power Transfer of both Artificial Intelligence and Industry 4.0 for Greater Autonomy. 2018. 23-34.

[15] W. Zhang and C. C. Mi, "Compensation Topologies of High-Power Wireless Power Transfer Systems," in IEEE Transactions on Vehicular Technology, vol. 65, no. 6, pp. 4768-4778, June 2016.

[16] C. Fang, J. Song, L. Lin and Y. Wang, "Practical considerations of series-series and series-parallel compensation topologies in wireless power transfer system application," 2017 IEEE PELS Workshop on Emerging Technologies: Wireless Power Transfer (WoW), Chongqing, 2017, pp. 255-259.

[17] Qiu, Chun & Chau, K.T. & Wood Ching, Tze & Chunhua, Liu. (2014). Overview of Wireless Charging Technologies for Electric Vehicles. Journal of Asian Electric Vehicles. 12. 1679-1685. 10.4130/jaev.12.1679

[18] Qualcomm Halo Wireless Electric Vehicle Charging, (2018,september12) available: https://www.qualcomm.com/solutions/automotive/wevc

[19] R. Nasiri, M. Khayamy, M. Rashidi, A. Nasiri and V. Bhavaraju, "Optimal Solar PV Sizing for Inverters Based on Specific Local Climate," 2018 IEEE Energy Conversion Congress and Exposition (ECCE), Portland, OR, 2018, pp. 6214-6219.

[20] M. Rashidi, A. Bani-Ahmed, R. Nasiri, A. Mazaheri and A. Nasiri, "Design and implementation of a multi winding high frequency transformer for MPSST application," 2017 IEEE 6th International Conference on Renewable Energy Research and Applications (ICRERA), San Diego, CA, 2017, pp. 491-494

[21] M. Rashidi, A. Bani-Ahmed and A. Nasiri, "Application of a multi-port solid state transformer for volt-VAR control in distribution systems," 2017 IEEE Power & Energy Society General Meeting, Chicago, IL, 2017, pp. 1-4

[22] M. Rashidi, M. Sabbah, A. Bani-Ahmed, A. Nasiri and M. H. Balali, "Design and implementation of a series resonant solid state transformer," 2017 IEEE Energy Conversion Congress and Exposition (ECCE), Cincinnati, OH, 2017, pp. 1282-1287

[23] M. Rashidi, A. Nasiri and R. Cuzner, "Application of multi-port solid state transformers for microgrid-based distribution systems," *2016 IEEE International Conference on Renewable Energy Research and Applications (ICRERA)*, Birmingham, 2016, pp. 605-610

[24] N. Mohan, T. Undeland and W. Robbins “Power Electronics : Converters, Applications, and Design” Third Edition, 2003 PP252

[25] C. Buccella, C. Cecati, H. Latafat and K. Razi, "Digital control of a half-bridge LLC resonant converter," *2012 15th International Power Electronics and Motion Control Conference (EPE/PEMC)*, Novi Sad, 2012, pp. LS6a.4-1-LS6a.4-6.

[26] Sam Abdel-Rahman “Resonant LLC Converter: Operation and Design 250 W 33 Vin 400 Vout Design Exam”, Infineon Technologies North America (IFNA)

[27] Control of Unit Power Factor PWM Rectifier,"Meifang Xue, Mingzhi He School of Electrical Engineering, Beijing Jiaotong University, Beijing, China Email: xuemeifang12@gmail.com